

Response to Comments of Reviewer #2

Referee comments are in black. Author responses are in blue.

General comments: Tibetan Plateau (TP) plays a very important role in East Asian climate. Perturbation in thermodynamic fields of the Qinghai-Xizang Plateau by anthropogenic or natural aerosols might induce substantial regional climate changes and serious air pollutions. However, the variations of aerosols in TP region are less known compared with those in East or South Asian regions. This study investigates the characteristics and potential sources of aerosols in TP based on ground-based and satellite observations as well as numerical models. The results are interesting and they may help us better understanding the temporal and spatial variations of the aerosols in TP and subsequently the aerosol climate effects in Asian region. The topic of this study is novel to some degrees. And the paper has a potential for publication in the journal after revisions.

Response: Thanks a lot for your important comments and suggestions. We have made our best efforts to modify the manuscript according to your comments and suggestions.

Comments:

1. Introduction should be re-organized to a degree to make it more readable and more clearly.

Response: We have tried our best to re-organized the introduction and added some statements to make it more clearly, including as followed:

Moved the last four lines of first paragraph to the beginning of fourth paragraph in the revised version.

Separated the shortage of current study and the subject of this work (the third paragraph of the origin version), and added some sentences to show the research background in the third paragraph.

Added a connection sentence before the citation of Lau et al. (2006), i.e., “*The increase in aerosols over the TP may have an important impact on the regional or global climate.*”

Moreover, this paper has been edited by native English speakers to make it more readable.

2. The authors should make some comparisons of aerosol optical properties which derive from different platforms when investigating the temporal and spatial variations of aerosols in TP region.

Response: Thanks for this suggestion. We have added the comparison of aerosol optical properties between MODIS and CE318 sunphotometer in revised version at section 3.2 as following:

“

Ground-based observations can offer accurate aerosol optical properties at point locations but lack spatial coverage. The MODIS aerosol product can provide the spatial variation in AOD over the TP. Thus, we evaluated the MODIS_AOD using the ground-based observation CE318_AOD at 550 nm over the TP sites. The CE318_AOD at 550

nm was interpolated from 440 nm, 675 nm, 870 nm and 1020 nm by using an established fitting method from Ångström (1929). The matchup method was that the CE318 data within 1 hour of the MODIS overpass were compared with the MODIS data within a 25 km radius of the ground-based site. The minimum requirement for a matchup was at least 3 pixels from MODIS.

Figure 5 shows the results of MODIS_AOD compared to the collocated ground CE318 observations over the TP. There are 996 instantaneous matchups of Terra and Aqua MODIS during the CE318 instrument measurement period at the five TP sites. The MODIS_AOD overestimates the AOD at 550 nm with a positive mean bias of 0.02 and a root mean squared error (RMSE) of 0.11. The RMSE value is lower than that of the North China Plain sites (~0.25) (Bilal et al., 2019). The slope and intercept of the best-fit equation between the MODIS_AOD and CE318_AOD at 550 nm are 0.46 and 0.06, respectively, with a correlation coefficient (R) of 0.54. There are 67.8% of the compared AODs within the expected error envelope of $0.05 + 0.15AOD$ (%EE). The R value is lower than that in the global assessment statistics, while the %EE is higher than that in the global evaluation (Bilal and Qiu, 2018). Overall, the results suggest that the MODIS_AOD product can be used to study the aerosol spatial variation over the TP region.

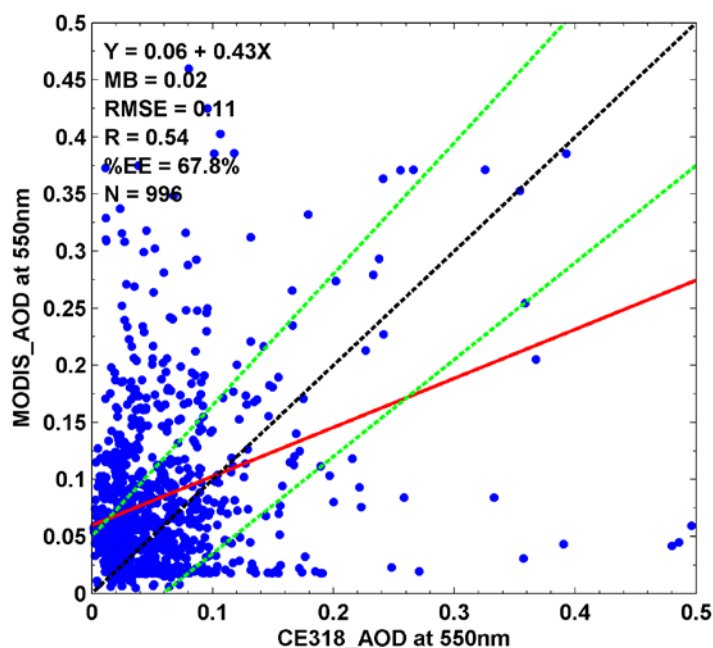


Figure 5. Comparisons of the 550 nm AOD measured by the CE318 instrument (CE318_AOD) over Tibetan Plateau stations with the MODIS retrieval Deep-Blue/Dark-Target combined AOD of 10 km spatial resolutions (MODIS_AOD). The statistical parameters in this figure include the number of matchup data (N), the slope and intercept at the y-axis of linear regression (read line), the mean bias (MB), root mean squared error (RMSE), correlation coefficient (R), and the percentage of data within the expected error $0.05 + 0.15AOD$ (%EE) which is used as the MODIS AOD expected uncertainty over land (green lines).”

3. A more detailed description on the accuracy of each type of platform data is needed. Does MODIS products accurate enough in bright surface (such as in desert region in TP)?

Response: The accuracy of the data from ground-based CE318 instruments was shown in section 2.2.1, and we have added the calibration and data control in section 2.2.1, i.e., *“The instruments were periodically calibrated using the Langley method at AERONET global calibration sites (the Izaña, Spain or the Mauna Loa, USA) or using the inter-comparison calibration method at the Beijing-CAMS site (Che et al., 2015). The cloud-screened and quality-controlled data of AOD, ...”*

For CALIOP data, the data version is specified (*“version 4.10”*) and a reference of data assessment has been cited in section 2.2.3, i.e., *“Kumar et al. (2018) have showed that the AOD from CALIOP version 4.10 agreed with the ground-based CE318 observation at a site in the central Himalayas with a correlation > 0.9 and ~ 87 % matchup data were within the expected error.”*

For the MODIS data, we used the MODIS Collection 6 Deep-Blue (DB)/ and Dark-Target (DT) combined AOD at 550 nm product. The description of this product has been added as followed: *“The MODIS AOD at 550 nm (MODIS_AOD) combined the DT and DB algorithms merges the products from the two algorithms based on the normalized difference vegetation index (NDVI) statistics as follows: 1) the DT AOD data are used for NDVI > 0.3; 2) the DB AOD data are used for NDVI < 0.2; and 3) the mean of both the algorithms or AOD data with high quality flag are used for $0.2 \leq NDVI \leq 0.3$.”* Thus, the MODIS DT-DB AOD used the value from DB algorithm in bright surface, which algorithm is regarded as the better retrieval of AOD in bright surface than DT algorithm. In addition, we have added the evaluation of MODIS products using the ground CE318 sunphotometer observations, and the results showed that 67.8% of the compared AODs were within the expected error envelope of 0.05+0.15AOD. The content that added in section 3.2 can be seen in the response of comment 2.

4. Validation of GEOS-Chem is need. The authors should compare the simulated aerosols with the observations.

Response: The simple comparison between model simulated AOD and ground observed AOD was shown in figure 13. We wanted to validate the GEOS-Chem using MODIS AOD, but MODIS AOD products were almost unavailable over The TP for the cloud contamination during the case period. We have not data of observed chemical component, so this evaluation can not be conducted. But according this suggestion, we have added more evaluated parameters between model and CE318 observed data in the third paragraph of section 5 and the figure is updated in the revised version as followed: *“The evaluation results showed that the model underestimated the daily AOD at the three sites during this period, with negative mean biases from -0.28 to -0.08. However, the Model_AOD was relatively high correlated with the CE318_AOD at 550 nm, with*

the R values of 0.61 at Lhasa, 0.89 at NAM_CO and 0.86 at QOMS_CAS. These R values are higher than the model evaluation in South China and Indo-China Plain (~ 0.5) (Zhu et al., 2017).”

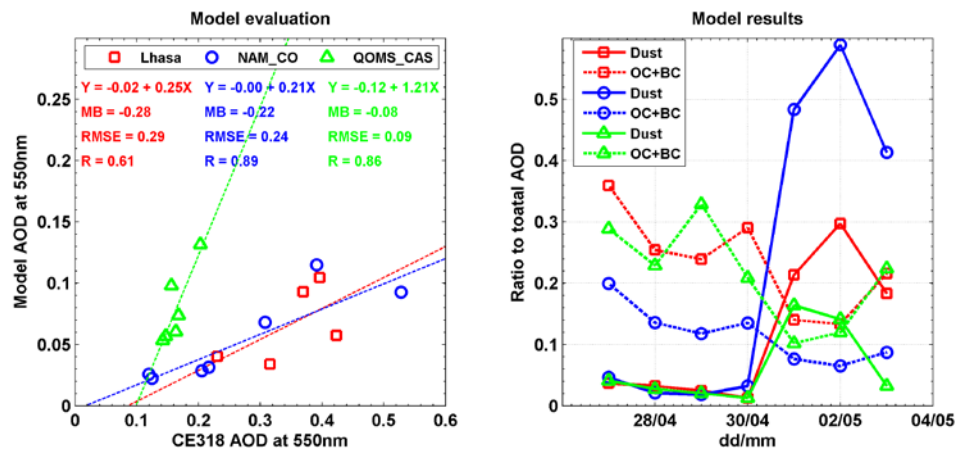


Figure 1. The GEOS-Chem model simulated the daily average AOD vs CE318 observed daily AOD at 550nm and the ratios of dust or organic carbon (OC) and black carbon (BC) aerosol to the total AOD during 27 April, 2016 – 3 May, 2016 at Lhasa, NAM_CO and QOMS_CAS. The statistical parameters used in Modal evaluation are the same as Figure 5.

5. How frequency of aerosol pollutions in Qinghai-Tibet Plateau based on your study?
Response: The frequencies of high aerosol loading ($AOD_{440\text{ nm}} > 0.4$) during the CE318 observation period were 1.57%, 1.79%, 0.21%, 0.42% and 0.11% at the Lhasa, Mt_WLG, Muztagh_Ata, NAM_CO, and QOMS_CAS site, respectively. These values are relatively low. But as one of the most pristine terrestrial regions of the Earth, the high aerosol loading over TP needs to be studied. The frequencies have been added in the revised version, i.e., “The frequencies of high aerosol loading ($CE318_AOD > 0.4$) during the CE318 measurements were 1.57%, 1.79%, 0.21%, 0.42% and 0.11% at the Lhasa, Mt_WLG, Muztagh_Ata, NAM_CO, and QOMS_CAS sites, respectively.”

6. A deeper discussion is needed in Results section, such as make some comparisons or summaries from similar studies.

Response: We have added some discussion by comparing to other studies, including but not limited to:

The comparison of AOD in Tibetan sites and other regional background sites in China is added in section 3.1.

“The annual averages of $CE318_AOD$ (shown in Figure 2) are 0.05-0.14 over TP sites. These average values are lower than those in other regional background sites, such as Longfengshan (0.35) in Northeast China (Wang et al., 2010), Xinglong (0.28) in North China Plain (Zhu et al., 2014), Lin’an (0.89) in Eastern China (Pan et al., 2010) and Dinghushan (0.91) in Southern China (Chen et al., 2014). The low aerosol loading over the five TP sites indicates excellent air quality over the TP region.”

The EAE in TP sites are compared with the inland urban and suburban sites in China

by adding the values of EAE.

“This size distribution explained the relative low annual averages of EAE at the five sites (all annual EAE in Figure 2 are less than <1.0), compared to the those at the inland urban and suburban sites in China (Xin et al., 2007), such as Beijing (1.19) (Fan et al., 2006), Nanjing (1.20) (Zhuang et al., 2018; Zhuang et al., 2017), Kunming (1.25) (Zhu et al., 2016), and Chengdu (1.09) (Che et al., 2015)”.

The results of the evaluation of MODIS AOD over TP are compared with the global and the other regional evaluations. See the response of comment 2.

The case study has been compared with another case study. The discussion of the difference from Jia et al. (2015) is added, i.e., *“Jia et al. (2015) has shown that the dust from India polluted by anthropogenic aerosols can be transported to the TP, but the back trajectories on 1 and 3 May illustrated that the airflows that ended at Lhasa were from the north or northwest rather than the south, indicating that the polluted dust over the TP on 3 May was more likely the mixing result of dust and smoke aerosol. In addition, the lengths of the back trajectories (especially the back trajectories at 10 m and 500 m above ground level) on 1 May showed that the airflows moved slowly, which allowed the possibility of aerosol mixture over the TP.”*

7. Conclusions should be shortened and more concise.

Response: The major conclusions have been refined as:

- “
- (1) *The annual CE318_AOD at most TP sites showed increasing trends (0–0.013/year) during the past decade. Increasing tendencies in the annual-averaged EAE were also found at most TP sites. Spatially, the MODIS_AOD showed negative trends in the northwest edge close to the Taklimakan Desert and the east of Qaidam Basin and slightly positive trends in most of the other areas of the TP.*
 - (2) *Different aerosol types and sources contributed to the high aerosol loading at the five sites: dust was dominant in Lhasa, Mt_WLG and Muztagh with sources from the Taklimakan Desert, but fine aerosol pollution was dominant at NAM_CO and QOMS_CAS with the transport from South Asia.*
 - (3) *A case of smoke followed by dust pollution at Lhasa, NAM_CO and QOMS_CAS during 28 April – 3 May 2016 showed that the smoke aerosol in South Asia was first uplifted to 10 km and transported to the centre of TP. Then, the dust from the Taklimakan Desert could climb the northern slope of the TP and be transported to the TP, allowing the dust and smoke aerosol over the TP to mix.*

8. English should be improved substantially throughout the whole manuscript.

Response: The revised paper has been improved by native English speakers.

1 **Marked-up Manuscript:**

2 **Spatiotemporal variation of aerosol and potential long-range** 3 **transport impact over Tibetan Plateau, China**

4 Jun Zhu^{1,2,3}, Xiangao Xia^{2,4}, Huizheng Che³, Jun Wang⁵, Zhiyuan Cong⁶, Tianliang
5 Zhao¹, Shichang Kang^{7,9}, Xuelei Zhang⁸, Xingna Yu¹, Yanlin Zhang¹

7 ¹ Collaborative Innovation Center on Forecast and Evaluation of Meteorological Disasters, Key
8 Laboratory for Aerosol-Cloud-Precipitation of China Meteorological Administration, Nanjing
9 University of Information Science and Technology, Nanjing 210044, China;

10 ² LAGEO, Institute of Atmospheric Physics, Chinese Academy of Sciences, Beijing 100029, China;

11 ³ State Key Laboratory of Severe Weather (LASW) and Key Laboratory of Atmospheric Chemistry
12 (LAC), Chinese Academy of Meteorological Sciences, CMA, Beijing, 100081, China;

13 ⁴ University of Chinese Academy of Sciences, Beijing, 100049, China;

14 ⁵ Center of Global and Regional Environmental Research and Department of Chemical and
15 Biochemical Engineering, University of Iowa, Iowa City, Iowa, USA;

16 ⁶ Key Laboratory of Tibetan Environment Changes and Land Surface Processes, Institute of Tibetan
17 Plateau Research, Chinese Academy of Sciences, Beijing 100101, China;

18 ⁷ State Key Laboratory of Cryospheric Science, Northwest Institute of Eco-Environment and
19 Resources, Chinese Academy of Sciences, Lanzhou 730000, China;

20 ⁸ Northeast Institute of Geography and Agroecology, Chinese Academy of Sciences, Changchun
21 130102, China;

22 ⁹ CAS Center for Excellence in Tibetan Plateau Earth Sciences, China.

24 Corresponding author: Jun Zhu (junzhu@nuist.edu.cn) & Xiangao Xia (xxa@mail.iap.ac.cn)

26 **Abstract:**

27 The long-term temporal-spatial variations ~~of~~ in the aerosol optical properties ~~in-over the~~ Tibetan
28 Plateau (TP) and the potential long-range transport from surrounding areas to TP were ~~analyzed~~
29 analysed in this work, by using multiple years of sunphotometer measurements (CE318) at five
30 stations in the TP, satellite aerosol production~~s~~ from the Moderate Resolution Imaging
31 Spectroradiometer (MODIS) and Cloud-Aerosol Lidar with Orthogonal Polarization (CALIOP),
32 back-trajectory analysis from the Hybrid Single-Particle Lagrangian Integrated Trajectory
33 (HYSPLIT) and model simulations ~~of-from~~ the Goddard Earth Observing System (GEOS)-Chem
34 chemistry transport model. The results from the ground-based observations show that the annual
35 aerosol optical depth (AOD) at 440 nm at most TP sites increased in ~~the-past~~ recent decades with
36 trends of 0.001 ± 0.003 /year at Lhasa, 0.013 ± 0.003 /year at Mt_WLG, 0.002 ± 0.002 /year at NAM_CO,
37 and 0.000 ± 0.002 /year at QOMS_CAS. The increasing trend ~~is-was~~ also found for the aerosol
38 Extinction Ångström exponent (EAE) at most sites, ~~except for~~ with the exception of the Mt_WLG
39 sites ~~with-an-obvious-decreasing-trend~~. Spatially, the AOD at 550 nm observed from MODIS ~~shows~~
40 showed negative trends ~~in-at~~ the northwest edge closed to the Taklimakan Desert and to the east of
41 the Qaidam Basin and slightly positive trends in most of the other areas of the TP. Different aerosol
42 types and sources contributed to the-a polluted day (with CE318 AOD at 440_nm > 0.4) ~~in-at~~ the

1 five sites ~~of~~on the TP: dust was dominant aerosol type in Lhasa, Mt_WLG and Muztagh with
2 sources ~~from~~in the Taklimakan Desert but fine aerosol pollution was dominant at NAM_CO and
3 QOMS_CAS with ~~the~~ transport from South Asia. A case of aerosol pollution at Lhasa, NAM_CO
4 and QOMS_CAS during 28 April – 3 May 2016 ~~reveals~~revealed that the smoke aerosols ~~in~~from
5 South Asia were lifted up to 10_km and transported to the TP, while the dust from the Taklimakan
6 Desert could climb the north slope of the TP and then be transported to the ~~center~~central TP. The
7 long-range transport of aerosol thereby seriously impacted ed the aerosol loading over the TP.

8 **Keywords:** Aerosol optical depth, Tibetan Plateau, aerosol pollution, long-range transport

1. Introduction

The heavy haze ~~that has~~ occurred in ~~past-recent~~ years in China ~~was-has been~~ largely attributed to the atmospheric aerosols (Zhang et al., 2015). ~~Besides~~In addition, atmospheric aerosols can affect the climate through the interactions between aerosol-radiation and between aerosol-cloud (Takemura et al., 2005; Li et al., 2017), while the clouds and its precipitation are also ~~in connection with the~~connected to large scale atmospheric circulations (Yang et al., 2010; Yang et al., 2017a). However, ~~there is still a high level of the~~uncertainty ~~of about~~ the impact of aerosols on the climate ~~effect is still high~~, which is mostly due to the highly spatiotemporal variability of aerosols. Therefore, ~~the study of studying the aerosol physical and chemical properties of aerosols over different regions is very essential. Ground-based measurements can offer more accuracy data of aerosol properties, while large-scale observation of aerosol optical and physical properties needs satellite remote-sensing method. Thus, long-term detection of aerosols from both of the ground and satellite platforms is absolutely necessary to improve understanding of the climate effects of aerosol.~~

The Tibetan Plateau (TP), is the largest elevated plateau in East Asia and considered as one of the most pristine terrestrial regions, ~~alongside along with~~ the Arctic and Antarctic. However, in the past two decades, ~~the~~ TP has been surrounded by ~~the an unprecedented-unprecedented~~ growing growth of emissions of Asian air pollutants from ~~the~~ various sources. Consequently, some ~~researches studies~~ have demonstrated that the aerosols transported from its around areas (South Asia and Taklimakan Desert) have polluted the TP (Huang et al., 2007; Xia et al., 2011; Kopacz et al., 2011; Lu et al., 2012; Liu et al., 2015). The increase in aerosols over the TP may have an important impact on the regional or global climate. Lau et al. (2006) has suggested that increased absorbing aerosols (dust and black carbon) over ~~the~~ TP may create a positive tropospheric temperature anomaly over ~~the~~ TP and adjacent regions to the south, causing the advance and enhancement of the Indian summer monsoon. ~~While a~~ Attempts ~~were-have been~~ made to reveal the linkages between ~~the~~ climate change (such as changes to glaciers and monsoons) and the air pollutants around ~~the~~ TP (mainly absorbing carbonaceous materials) (Qian et al., 2011; Wang et al., 2016; Lee et al., 2013). ~~However~~, the quantitative effect of the TP aerosol on climate variability remains largely unknown, and ~~there is an urgent need~~ it is very essential to fully understand the aerosol characteristics over ~~the~~ TP.

A large amount of attention has been paid to aerosol characteristics over the TP (Wan et al., 2015; Tobo et al., 2007; Zhao et al., 2013; Liu et al., 2008; Du et al., 2015). Although the seasonal variations in aerosol properties over the TP have been analysed based on ground-based observations or satellite products (Shen et al., 2015; Xia et al., 2008), analysis is needed of the long-term trends in the variation of aerosols over the TP to provide predictions and guidelines for environment policies. In past studies, spring or summer have often been studied due to the important impacts of dust and carbonaceous aerosols (Huang et al., 2007; Cong et al., 2007; Lee et al., 2013). However, most studies of the aerosol properties based on ground-based measurements have been conducted at a single site over the TP, such as NAM CO (Cong et al., 2009), Mt. Yulong (Zhang et al., 2012), and Mt. WLG (Che et al., 2011). ~~Past studies analyzing the aerosol variation in TP used ground-based observations and satellite products, but many of these~~ Past studies have mostly focused on ~~the~~ single stations or short-term variations due to the ~~difficulties difficulty to of take-taking a the~~ sufficient number of ground-based observations in challenging weather conditions over the remote plateau.

Ground-based measurements can offer more accurate data on aerosol properties, while large-scale spatial observations of aerosol optical and physical properties require satellite remote-sensing methods (Li et al., 2015; Li et al., 2018; Xing et al., 2017). Thus, the long-term detection of aerosols from both ground and satellite platforms is absolutely necessary for improving our understanding of the climate effects of aerosol over the TP region. Consequently, based on multiple years of observations from five ground-based sunphotometers at the TP and the MODIS aerosol optical depth product over the TP region, our work here is ~~to~~ focused on the long-term spatiotemporal-spatial variations ~~of in~~ the aerosol optical properties ~~over multiple stations~~ over the TP and the aerosol properties and sources during the high aerosol ~~pollution events~~ loading in over the TP based on multiple years of five ground-based sunphotometer observations and the MODIS aerosol optical depth product in TP. In addition, we ~~will~~ also combined the observation and models to study the aerosol transport process over the TP, thereby helping to reduce the uncertainties in estimate estimating ~~of~~ aerosol radiative forcing and aerosol sources.

In this paper, section 2 describes the observation sites, data and methods~~s~~~~are~~. The results of the analysis of the spatiotemporal-spatial variations ~~of in~~ aerosol properties over the TP ~~is are~~ shown in ~~Section~~ section 3. The analysis of aerosol ~~pollution~~ high loading and an aerosol transport case are presented in section 4 and 5, respectively. The conclusions are presented in section 6.

2. Site, data and ~~Methodology~~ methodology

2.1 ~~site~~ Sites

In this study, five sites in the TP equipped with ~~the~~ sun and sky scanning radiometers (CE318) were used (Figure 1). Table 1 shows the station locations and descriptions. Lhasa station is the only urban site ~~where that can~~ suffer from the local anthropogenic emissions. As ~~for~~ For the other four sites, local anthropogenic emissions are extremely rare due to ~~few signs~~ the low number of human habitation inhabitants. However, Mt_WLG is in the northeast of the TP, where it is situated at on the dust transport path from the maximal-largest desert ~~of in~~ China (the Taklimakan Desert). The Muztagh_Ata site is located in the northwest corner of the TP and beside-next to the Central Asian Deserts and the Taklimakan Desert. NAM_CO is located in on the central Tibetan Plateau, 220 km away from Lhasa. QOMS_CAS is located at the northern slope of Mt. Qomolangma on the border of Tibet and Nepal. Therefore, these five sites ~~can stand for~~ are representative of the spatial features of the TP.

2.2 Data

2.2.1 CE318 aerosol optical properties

The column-integrated aerosol properties over the five TP sites are derived from CE318 measurements. Table 1 ~~has showed~~ shows the observation period. The CE318 instrument measures direct solar spectral radiation and the angular distribution of sky radiance. These spectral radiances can be used to ~~retrieval~~ retrieve aerosol optical parameters (such as aerosol optical depth (AOD)) based on Beer's Law, ~~and~~ aerosol microphysical properties (such as volume size distribution) and ~~its the~~ radiative forcing features through radiation transfer theory (Dubovik and King, 2000; Dubovik et al., 2006). The instruments were periodically calibrated using the Langley method at AERONET global calibration sites (the Izaña, Spain or the Mauna Loa, USA) or using the inter-

comparison calibration method at the Beijing-CAMS site (Che et al., 2015). The cloud-screened and quality-controlled data of AOD, Extinction Ångström exponent (EAE), and aerosol volume size distribution ($dV(r)/d\ln r$) are used in this work (Giles et al., 2019). Eck et al. (1999) showed that the uncertainty of the AOD was ~~about~~ approximately 0.01 to 0.02. The EAE ~~is~~ was calculated from the AOD at 440 and 870 nm. The errors of retrieval for $dV(r)/d\ln r$ ~~are~~ were less than 10% in the maxima of the $dV(r)/d\ln r$ and may increase up to 35% for the minimum values of $dV(r)/d\ln r$ within the radius range between 0.1 μm and 7 μm ; for the edges of the retrieval size, the errors increased apparently, ~~which does~~ but did not significantly affect the derivation of the main feature of $dV(r)/d\ln r$ (Dubovik et al., 2002).

2.2.2 The MODIS AOD product

The Moderate Resolution Imaging Spectroradiometer (MODIS) instrument is a multi-spectral sensor with a wide spectral range from 0.4 to 14.4 μm in 36 wavelength bands, onboard the Terra (morning descending directions) and Aqua (afternoon ascending directions) satellites in polar orbit, respectively. Its broad swath of 2330 km permits retrieval aerosol products to cover the global word within 1-2 days. In this study, both Terra and Aqua MODIS Collection 6 Deep-Blue (DB) and Dark-Target (DT) combined AOD at 550 nm product with 10 km spatial resolution (~~MODIS_AOD~~) (Levy et al., 2013) from 2006 to 2017 ~~are~~ were used. The MODIS AOD at 550 nm (MODIS_AOD) combined the DT and DB algorithms merges the products from the two algorithms based on the normalized difference vegetation index (NDVI) statistics as follows: 1) the DT AOD data are used for $\text{NDVI} > 0.3$; 2) the DB AOD data are used for $\text{NDVI} < 0.2$; and 3) the mean of both the algorithms or AOD data with high quality flag are used for $0.2 \leq \text{NDVI} \leq 0.3$. The MODIS_AOD has been widely validated in the global or regional areas (Bilal et al., 2018; Ma et al., 2016; Sayer et al., 2014). The root-mean-square error of MODIS_AOD was about 0.13, and the percentage of MODIS_AOD data within the expected error was ~~larger~~ more than 71% at the Kunming site, which ~~around~~ is near the TP (Zhu et al., 2016).

2.2.3 The CALIOP profile data

The Cloud-Aerosol Lidar with Orthogonal Polarization (CALIOP), the primary instrument on board of CALIPSO satellite, is a near-nadir viewing two wavelength (532 nm and 1064 nm) polarization-sensitive lidar ~~which~~ that performs global vertical profiles measurements of aerosols and clouds (Winker et al., 2010). It provides three primary calibrated and geolocated profile products ~~of profiles~~: total attenuated backscatter at 532 nm and 1064 nm and the perpendicular polarization component at 532 nm. The ~~data~~ CALIOP (version 4.10) products used in this study include the attenuated backscattering coefficient profiles from ~~level~~ Level 1B and the vertical feature mask data products of aerosol subtype from level 2 products under 15 km altitude, which ~~are~~ were downloaded from the Langley Atmospheric Science Data Center (ASDC). Kumar et al. (2018) have showed that the AOD from CALIOP version 4.10 agreed with the ground-based CE318 observation at a site in the central Himalayas with a correlation > 0.9 and $\sim 87\%$ matchup data were within the expected error.

2.3 Methodology

The ground-based CE318 observations and MODIS AOD products ~~are~~ were analyzed-analysed

1 to show the spatiotemporal-spatial variations of in aerosol properties in TP.

2
3 The CE318 observed AOD at 440 nm with values larger than 0.4 at each site is-was-considered
4 as specially analysed to study the aerosol properties of the high aerosol pollution-loading over the
5 TP. The value of 0.4 was selected because the mean annual values of AOD observed by CE318
6 instruments at the TP sites were less than ~0.1 in the past studies (Xia et al., 2016; Cong et al., 2009),
7 and this value is normally regarded as the high aerosol loading (Eck et al., 2010; Giles et al., 2012).
8 The bBack trajectories are-were used for the aerosol source analysis in the TP. The bBack trajectories
9 for-on the high aerosol pollution-loading study-days are-were calculated by using the Hybrid Single-
10 Particle Lagrangian Integrated Trajectory (HYSPPLIT) model which is driven by the one degree
11 horizontal resolution archived meteorological fields with (Draxler and Hess, 1998). 72-hour back
12 trajectories ending at the five sites at 10 m above ground level at 12 UTC on the days of-with high
13 aerosol pollution-loading (AOD at 440 nm >0.4) are-were used to identify the air mass sources.

14
15 A Case case study of long-range aerosol transport to the TP is-was selected based on the ground
16 CE318 observations over Lhasa, NAM_CO and QOMS_CAS. By-combing-The HYSPPLIT back
17 trajectories, and the MODIS and CALIOP products were used to show the potential aerosol sources,
18 spatial aerosol loading and the vertical features of the aerosol over the TP during the case period.
19 In addition, and the Goddard Earth Observing System (GEOS)-Chem chemistry transport model,
20 was used to simulate the AOD and its components (dust and carbon aerosol) during the case period,
21 which may reflect the change in aerosol type during the case period.the aerosol source and type
22 during the case is analyzed.

23
24 The GEOS-Chem chemical transport model (version 11-01) coupled with the online radiative
25 transfer calculations (RRTMG) at $0.5^\circ \times 0.667^\circ$ horizontal resolution over the East Asia domain
26 (Bey et al., 2001; Wang et al., 2004) is-was used-to-simulate-aerosol-variation-during-the-case-period.
27 The model was driving by the Global Modeling and Assimilation Office (GMAO) MERRA-2
28 meteorology with the temporal resolution of 3 hours for meteorological parameters and 1 hour for
29 surface fields. The simulation type of full chemistry in the troposphere was selected. The
30 implementation of RRTMG in GEOS-Chem was described in Heald et al. (2014). The AOD was
31 calculated according to Martin et al. (2003). The default global anthropogenic emissions were
32 overwritten over East Asia by the MIX inventory from Li et al. (2014). The Global Fire Emission
33 Database (GFED) (van der Werf et al., 2010) has been used to specify emissions from fire. The
34 default-More details on the configuration-schemes-respectively-for-advection,transport,convection,
35 deposition,model and the other emissions data used and the evaluation of AOD in the east and south
36 of the TP were shown in Zhu et al. (2017).
37 -are-used-for-the-model-simulation-of-full-chemistry.

38 In this study, the AOD from the CE318, MODIS, and GEOS-Chem model were used. For
39 convenience, CE318 AOD, MODIS AOD, and Model AOD stand for the AOD observed by
40 CE318, MODIS, and the AOD simulated by the GEOS-Chem model, respectively. For
41 CE318 AOD, the 440 nm wavelength is often studied, while MODIS AOD and Model AOD
42 generally use the data at 550 nm wavelength. Thus, unless otherwise specified, CE318 AOD,
43 MODIS AOD, and Model AOD hereinafter represent the ones at 440 nm, 550 nm, and 550 nm,
44 respectively.

3. Temporal-spatial variations of aerosol properties

3.1 Temporal variation of aerosol properties observed by the CE318 instruments

The monthly, seasonal, and annual variations in aerosol properties observed from the CE318 instruments at the five TP sites were analyzed.

Annual variation of CE318 AOD and EAE over TP at the four sites, i.e. Lhasa, Mt_WLG, NAM_CO, and QOMS_CAS are shown in Figure 2. The data of the CE318 observation at Muztagh_Ata site are available only during 2010, thus the annual variation at this site is not shown here. The annual AOD shows increased trends of $0.001 \pm 0.003/\text{year}$ at Lhasa, $0.013 \pm 0.003/\text{year}$ at Mt_WLG, and $0.002 \pm 0.002/\text{year}$ at NAM_CO during CE318 observed period. Mt_WLG site shows the most obvious increase of AOD during 2009–2013. These indicate the increase of aerosol loading in the three sites. The long term annual variation of AOD at QOMS_CAS is very small ($0.000 \pm 0.002/\text{year}$), but there still exists short term annual variation (decreased from 2010 to 2013 and increased from 2013 to 2016). The annual trends of EAEs show more evident than the AOD in these four sites. Most sites show the increased tendency of annual averaged EAE, except for Mt_WLG sites with a large decreasing trend of $-0.318 \pm 0.081/\text{year}$. This showed the size of aerosol at Mt_WLG sites increased, while the size of aerosol decreased in other three sites. Combining the AOD and EAE, the positive trend of AOD with the positive trend of EAE in the long term at most sites over TP indicates the addition of fine mode aerosol mainly from the anthropogenic impact. But in the short term, the increase of annual averaged AOD is often with the decrease of EAE over TP, which suggests the addition of coarse mode aerosol during the CE318 observation.

The monthly and seasonal statistics variations of CE318 AOD and EAE at the five sites over the TP are shown in Figure 3 and Table 2, respectively. Distinct monthly and seasonal variability of the AOD and EAE over the five sites can be found. The monthly mean CE318 AOD shows the highest value in April at the Lhasa (0.19), NAM_CO (0.09) and QOMS_CAS (0.10) sites, while the value at Mt_WLG was highest in June (0.20). The monthly mean CE318 AOD rapidly increases from January to April, and then slightly decreases to until December at the Lhasa, NAM_CO and QOMS_CAS sites. However, the monthly mean CE318 AOD at Mt_WLG shows almost symmetry is nearly symmetrical form from January to December. The monthly variation of EAE is different from the AOD at each site. The highest monthly EAE values occurs in September at Lhasa (1.15), October at Mt_WLG (1.15) and in January at the NAM_CO (0.93) and QOMS_CAS (0.17) sites. The EAE at QOMS_CAS also shows a high value of 0.17 in April, which may be caused by the smoke aerosol transported from South Asia during this period. The monthly mean EAE first decreases firstly from January to March, and then increases to until September at Lhasa. The monthly mean EAE values at NAM_CO also decreases from January to March, but does not increase apparently in the followed following months. The EAE at Mt_WLG shows a decreases from January to May and then increases obviously from May to October. The Lhasa, NAM_CO, and QOMS_CAS sites are near and located in the south of the TP. Thus, the variations of the aerosol properties in at these three sites are similar. The Mt_WLG site is located in the northeast of the TP, which is different from the southern sites. The Muztagh_Alt is in the northwest of the TP and is the nearest closest site to the Taklimakan desert. Desert, which causes the high AOD there (a few observed data may be another reason).

Looking at ~~Combining~~ the monthly CE318 AOD and EAE values together, ~~the~~ high CE318 AOD is often accompanied by ~~the~~ low EAE at Lhasa, Mt_WLG and NAM_CO, indicating that these sites suffered from ~~the~~ coarse aerosols such as dust (Huang et al., 2007; Liu et al., 2015; Zhang et al., 2001). However, ~~the~~ QOMS_CAS sites show ~~the~~ high CE318 AOD and high EAE at in April, which ~~is~~ may be related to ~~the~~ smoke aerosols transported from South Asia.

Table 2 shows the seasonal statistics of CE318 AOD and EAE. A distinct seasonal variation in CE318 AOD and EAE ~~variation~~ can be found over ~~the~~ TP sites. ~~The CE318 AOD~~ mean values in fall (SON) and winter (DJF) are lower at all sites except Muztagh. Muztagh_Ata shows high CE318 AOD in both observed seasons. Except for that in Muztagh, the ~~maximal~~ maximum seasonal CE318 AOD is observed in spring (MAM) (Lhasa, NAM_CO, and QOMS_CAS) or in summer (JJA) (Mt_WLG). The ~~minimal~~ minimum seasonal EAE occurred in spring (Lhasa, NAM_CO and Mt_WLG) or summer (QOMS_CAS), while ~~the maximal~~ maximum EAE values is ~~are~~ mostly observed in fall (Lhasa and Mt_WLG) and winter (NAM_CO and QOMS_CAS). These indicate frequently dust events over ~~the~~ TP in ~~the~~ spring period at Lhasa, NAM_CO and Mt_WLG. Mt_WLG is situated at on the dust transport path from the Taklimakan Desert, which causes the high CE318 AOD observed in spring and summer ~~in~~ at this site.

The seasonal size distributions of the five sites in ~~Figure 3~~ Figure 4 also demonstrate that coarse mode aerosol is dominant at the five TP sites in almost all seasons, which is different from ~~those in~~ the eastern pollution regions of China ~~with fine mode aerosol dominant~~, such as Yangtze River Delta, where fine mode aerosol is dominant (Zhuang et al., 2018). ~~These~~ This size distribution explained the relatively lower annual averages of EAE ~~in~~ at the five sites (all annual ~~EAE in Figure 2 are~~ less than <1.0), ~~which was lower than~~ compared to the ~~those at the~~ inland urban and suburban sites in China (Xin et al., 2007), ~~for the example of such as~~ Beijing (1.19) (Fan et al., 2006), Nanjing (1.20) (Zhuang et al., 2018; Zhuang et al., 2017), Kunming (1.25) (Zhu et al., 2016), and Chengdu (1.09) (Che et al., 2015). What's more, spring is the season with a high ~~high~~ volume concentration of coarse mode aerosol. Among the five sites, the southernmost sites, QOMS_CAS, showed the highest mean EAE and the size distribution was distinctly bimodal, especially in spring. This was also because of the frequently biomass burning activity in India and Nepal, which can transport the fine aerosol to the QOMS_CAS site.

The annual averages of CE318 AOD (shown in Figure 2) are 0.05-0.14 over TP sites. These average values are lower than those in other regional background sites, such as Longfengshan (0.35) in Northeast China (Wang et al., 2010), Xinglong (0.28) in North China Plain (Zhu et al., 2014), Lin'an (0.89) in Eastern China (Pan et al., 2010) and Dinghushan (0.91) in Southern China (Chen et al., 2014). The low aerosol loading over the five TP sites indicates excellent air quality over the TP region.

However, the aerosol loading at the TP sites presents interannual changes. The annual variations in CE318 AOD and EAE over TP at the four sites, i.e. Lhasa, Mt_WLG, NAM_CO, and QOMS_CAS are shown in Figure 4. The data for the CE318 observations at Muztagh_Ata site are only available for 2010; thus, the annual variation at this site is not shown here. The annual

CE318 AOD shows increasing trends of $0.001 \pm 0.003/\text{year}$ at Lhasa, $0.013 \pm 0.003/\text{year}$ at Mt. WLK, and $0.002 \pm 0.002/\text{year}$ at NAM CO during the CE318 observation period. The Mt. WLK site shows the most obvious increase in CE318 AOD during 2009-2013. These results indicate an increase in aerosol loading at the three sites. The long-term annual variation of CE318 AOD at QOMS CAS is very small ($0.000 \pm 0.002/\text{year}$), but there are still short-term annual variations (the values decreased from 2010 to 2013 and increased from 2013 to 2016). The annual trends of EAEs are more evident than the CE318 AOD at these four sites. Most sites show an increasing tendency in the average annual EAE except for Mt. WLK site, which shows a large decreasing trend of $-0.318 \pm 0.081/\text{year}$. This shows that the size of aerosol at the Mt. WLK site increased, while the size of the aerosol decreased in the other three sites. Looking at the CE318 AOD and EAE values together, the positive trend of CE318 AOD and the positive trend of EAE in the long term variation at most sites over TP indicates the addition of fine mode aerosol which may be related to the anthropogenic impact or long-distance transport of dust to the TP. However, in the short term, the increase in the average annual CE318 AOD is often associated with the decrease in EAE over the TP, which suggests the addition of coarse mode aerosol during the CE318 observation period.

3.2 Spatial variation of aerosol properties from MODIS

Ground-based observations can offer accurate aerosol optical properties at point locations but lack spatial coverage. The MODIS aerosol product can provide the spatial variation in AOD over the TP. Thus, we evaluated the MODIS AOD using the ground-based observation CE318 AOD at 550 nm over the TP sites. The CE318 AOD at 550 nm was interpolated from 440 nm, 675 nm, 870 nm and 1020 nm by using an established fitting method from Ångström (1929). The matchup method was that the CE318 data within 1 hour of the MODIS overpass were compared with the MODIS data within a 25 km radius of the ground-based site. The minimum requirement for a matchup was at least 3 pixels from MODIS.

Figure 5 shows the results of MODIS AOD compared to the collocated ground CE318 observations over the TP. There are 996 instantaneous matchups of Terra and Aqua MODIS during the CE318 instrument measurement period at the five TP sites. The MODIS AOD overestimates the AOD at 550 nm with a positive mean bias of 0.02 and a root mean squared error (RMSE) of 0.11. The RMSE value is lower than that of the North China Plain sites (~ 0.25) (Bilal et al., 2019). The slope and intercept of the best-fit equation between the MODIS AOD and CE318 AOD at 550 nm are 0.46 and 0.06, respectively, with a correlation coefficient (R) of 0.54. There are 67.8% of the compared AODs within the expected error envelope of $0.05 + 0.15\text{AOD}$ (%EE). The R value is lower than that in the global assessment statistics, while the %EE is higher than that in the global evaluation (Bilal and Qiu, 2018). Overall, the results suggest that the MODIS AOD product can be used to study the aerosol spatial variation over the TP region.

The spatial distribution of MODIS the annual MODIS AOD is shown in Figure 6. The MODIS AOD agrees with the CE318 AOD at 550 nm observed by CE318 at the five TP sites. The northwest area around the Taklimakan Desert and the northern part of the TP on the transport path of the Taklimakan Desert dust showed the high MODIS AOD (>0.25) in past-recent decades. In addition, the southern edge performed slightly high MODIS AOD (0.2-0.25) influenced by the aerosol transport from

South Asia. There ~~exists-is~~ some ~~little-small~~ area with high ~~MODIS_AOD~~AOD (~ 0.2) in the ~~center~~ ~~centre~~ of ~~the~~ TP, and the southeast region ~~is-shown-of~~shows low ~~MODIS_AOD~~AOD (~ 0.1), which may be attributed to the aerosol transport and surface features such as ~~vegetable-vegetation~~ cover, since there are few inhabitants. The seasonal departure of ~~MODIS-MODIS~~ AOD (Figure 7Figure 6) shows that high positive ~~MODIS_AOD~~AOD departure often appears in spring, especially for the northwest edge, north~~ern~~ area and south~~ern~~ edge of TP, which was ~~a~~ result ~~from-of~~the aerosol transport from the frequent dust events ~~at-in the~~ Taklimakan ~~Desert~~ and ~~the~~ fire activities in South Asia in spring.

A linear regression ~~trend~~ analysis of ~~the trends in~~ ~~MODIS~~-annual ~~MODIS_AOD~~AOD at 550nm over ~~the~~ TP from 2006 to 2017 was conducted using the least squares method. The spatial distribution of ~~the~~ annual trends in ~~MODIS-MODIS~~ AOD during 2006-2017 is illustrated in Figure 8Figure 7. There are no statistically significant trends in most areas during 2006-2007. The ~~MODIS_AOD~~AOD ~~performed-showed~~ negative trends in the northwest edge closed to ~~the~~ Taklimakan Desert and ~~to~~ the east of the Qaidam Basin and slightly positive trends in most of the other areas. The ~~areas where MODIS_AOD~~AOD ~~descending-decreased~~ ~~area-is~~ ~~are~~ mainly ~~located~~ ~~the-place~~ near the desert or ~~lied-in-on~~ the transport path of ~~the~~ desert dust. This descending trend may be related to the significant reduction in dust emissions caused by the decline in wind speed in recent years (Yang et al., 2017b). The positive trend in other most areas may be due to the rapid increase in human activities, such as the ~~expend~~expansion of tourism to ~~the~~ TP and ~~the~~ biomass burning in South Asia.

The seasonal trends ~~of-in~~ ~~MODIS-MODIS~~ AOD at 550 nm over ~~the~~ TP during 2006-2017 ~~is~~ ~~are~~ presented in Figure 9Figure 8. The spring showed the most obvious ~~of-the~~ decline in ~~MODIS_AOD~~AOD ($\sim 0.02/\text{year}$) ~~in-at~~ the north~~ern~~ edges and northeast part of ~~the~~ TP during 2006-2017, which also suggested ~~that~~ the reduction ~~of-in~~ dust impact from the Taklimakan Desert ~~as-like~~ the trend ~~of-in the~~ annual ~~MODIS-MODIS~~ AOD (seen in Figure 8Figure 7). In summer, the positive trend ~~of-in~~ ~~MODIS_AOD~~AOD over ~~the~~ TP was relatively apparent, and most higher sporadic positive values of ~ 0.01 occurred in ~~the~~ central and south~~ern~~ part of ~~the~~ TP. Summer is the tourist season ~~over-in the~~ TP and ~~the~~ tourism has developed in past decades, which may be one of the reasons ~~of-for~~ the higher positive trend in summer in ~~the~~ TP. The ~~apparent~~ positive trends in autumn and winter were relatively ~~less-lower~~ than ~~those in~~ summer, and ~~the~~ most positive trends were located at the northern TP. The reason ~~of-for~~ this phenomenon needs to be explored.

4. ~~Aerosol properties and potential sources during high aerosol loading~~Aerosol pollution at Tibetan plateau

The ~~annual~~ mean AOD in ~~the~~ TP is normally low ~~for its little trace-of~~due to the few human ~~inhabitants~~tion and high altitude. However, some high ~~CE318~~ AODs ~~with-values~~ larger than 0.4, ~~which is normally regarded as high aerosol loading~~ (Eck et al., 2010; Giles et al., 2012), ~~had been~~were observed at the five sites in ~~the~~ TP by CE318. ~~Thus, the CE318_AOD larger than 0.4 over TP can be considered as the aerosol pollution. The frequencies of high aerosol loading (CE318_AOD > 0.4) during the CE318 measurements were 1.57%, 1.79%, 0.21%, 0.42% and 0.11% at the Lhasa, Mt_WLG, Muztagh_Ata, NAM_CO, and QOMS_CAS sites, respectively. The aerosol properties and sources of-the-high-AOD(>0.4)during high aerosol loading in the TP need to be~~

studied.

Figure 10 shows the ~~CE318_AOD~~AOD with values larger than 0.4 versus EAE observed by CE318 at the five sites in the TP. Except for the Lhasa and Mt_WLG sites, almost all values of ~~CE318_AOD~~AOD are less than 1.0, which reflects the relatively clear environment over the TP. The EAE shows two ~~centers-centres~~ of at ~ 0.1 and ~ 1.5 . The low EAE (~ 0.1) ~~center-centre~~ is related to ~~the~~ dust events, which can cause higher concentrations of coarse particles in the atmosphere. Besides, most values of the low EAE (< 0.5) part are less than 0.2 (only a few of EAEs between 0.2-0.5 ~~is-are~~ observed at Lhasa and Mt_WLG), indicating that the pure dust type is more common than the polluted dust type in the TP according to Eck et al. (2010). The high EAE ~~center-centre~~ ~~in-at~~ ~ 1.5 indicates ~~the~~ mainly small sub-micron radius particles, which ~~is-can be~~ attributed to ~~the~~ anthropologic emissions. ~~There can be found that~~ the values of EAE > 1.0 ~~part-at~~ the NAM_CO and QOMS_CAS sites are generally higher than those at the Lhasa and Mt_WLG sites. According to ~~the~~ past studies, the EAE of biomass burning aerosol is generally higher than the urban/industry aerosol (Giles et al., 2012; Eck et al., 2010), which may cause the higher EAE at NAM_CO and QOMS_CAS (more biomass burning aerosol) than at Lhasa and Mt_WLG (more urban/industry aerosol). On the other hand, the values ~~with-in~~ the middle range of 0.5-1.0 ~~is-are~~ rare, indicating the less mix of ~~nature-natural~~ and human sources. The percentage of EAE bins to the number of ~~CE318~~CE318 AOD > 0.4 is distinct ~~from each other sites~~ (Table 3). The percentage of EAE < 0.5 is high than that of EAE > 1.0 at Lhasa, Mt_WLG and Muztagh_Ata, indicating more nature dust pollution than the ~~anthropologic-anthropogenic~~ pollution at these three sites. However, ~~more-a greater number~~ of high EAE values (> 1.0) ~~is-are~~ observed than EAE < 0.5 at the NAM_CO and QOMS_CAS sites, suggesting that ~~anthropogenic-anthropologic~~ pollution is more than ~~nature-natural~~ dust pollution at these two sites.

Figure 11 shows the aerosol size distribution binned by ~~CE318_AOD~~AOD at the five sites in the TP. The volume concentration of coarse mode particles increases more apparently than fine mode at Lhasa, Mt_WLG and Muztagh sites when the values of ~~CE318_AOD~~AOD increase. However, the size distribution at NAM_CO and QOMS_CAS shows the dominant ~~increasing~~increase of fine mode aerosol. These indicate of the different aerosol type pollution in these five sites: dust dominant in Lhasa, Mt_WLG and Muztagh and fine mode aerosol (mainly biomass burning aerosol) pollution dominant at NAM_CO and QOMS_CAS.

The dominant aerosol pollution type showed ~~the-obvious~~ distinctions ~~in-among~~ the five sites at on the TP, then where is the distinct aerosol pollution source at each site? We used the HYSPLIT back-trajectory model and the ~~MODIS-MODIS~~ AOD on the day with aerosol pollution day (~~CE318~~CE318 AOD > 0.4) to show the aerosol source on the pollution day at each site. Figure 12 shows the 72 hour back-trajectories ended at the five site (10 m above ground level) in the TP overlaid by ~~with~~ the mean ~~MODIS-MODIS~~ AOD at 550 nm on the aerosol pollution day observed by the ground-based CE318 (~~CE318-CE318~~ AOD > 0.4). The CE318 instruments have observed 78, 20, 2, 15, and 14 days with instantaneous AOD at 440 nm > 0.4 at Lhasa, Mt_WLG, Muztagh_Ata, NAM_CO and QOMS_CAS, respectively. The aerosol pollution days at Lhasa, Mt_WLG, and Muztagh_Ata observed by CE318 are often with low EAE (black trajectories). The airflows ended at the Lhasa site on the polluted days are mainly from the northwest and southwest. The MODIS

MODIS AOD around Lhasa in the area of the back-trajectories with CE318 EAE <0.5 passing does not show significantly high values, especially in the Taklimakan Desert, which indicates that the dust pollution at Lhasa is mainly from local or around-surrounding dust events rather than transport from the Taklimakan Desert. The Mt_WLG shows that the air mass on the pollution days comes from the west and east and the way-path of back trajectories is-with has high MODIS MODIS AOD. The high values of MODIS MODIS AOD has-shown shows two transport paths of dust aerosol to Mt_WLG: one is through the Qaidam Basin and another-the other is through the northeast edge of the TP. The two polluted days observed by CE318 at the Muztagh_Ata shows the easterly airflows originated-originating from the Taklimakan Desert. The direction of the back-trajectories of EAE<0.5 that ended at NAM_CO is similar to Lhasa, while the southerly air flows with high EAE (red trajectories) is originate from Nepal, where frequent biomass burning happened and caused the high MODIS MODIS AOD values. The trajectories ended at QOMS_CAS and the high MODIS MODIS AOD of its-passing the path has-shown revealed the the transport of smoke-finer aerosol from South Asia to this site.

5. Case study of long-range transport to the TP

The long-range transport of aerosol can cause the aerosol pollution and affect the long-term variation in aerosol over the TP. In addition, the dominant aerosol type may change at the TP sites during a case of aerosol transport. Thus, A-a specific case of aerosol pollution during 27 April - 3 May 2016 is-was analyzed-analysed further. This case is selected based on the observations of-from the CE318 instrument. During 28 April -1 May, the CE318 AODAOD-observed-by-CE318 at Lhasa, NAM_CO, QOMS_CAS sites showed up the values larger than 0.4, which value reached up to more than 3 times of the mean values of CE318 AODAOD of each site (0.11 at Lhasa, 0.05 at NAM_CO and QOMS_CAS). This is-was indicative of the aerosol pollution at the three sites. Then, how about the aerosol properties of this period and where did the polluted aerosol come from?

Figure 13Figure-12 shows the daily CE318 AODAOD and EAE during 27 April – 03 May at the three sites. The mean values of CE318 AODAOD-from-CE318-Sun-photometer were 0.45, 0.38, and 0.23 at Lhasa, NAM_CO and QOMS_CAS, respectively. These even reached to-4 times of the annual mean CE318 AODAOD at each site. The mean EAEs were 0.98, 1.22, and 1.44 at Lhasa, NAM_CO and QOMS_CAS, respectively, which was relative higher than the annual averages and suggested the fine aerosol entrance. There were CE318 AODAOD peaks at the three sites during 27 April – 03 May. Lhasa showed the-an increase of CE318 AODAOD from 0.30 on 27 April to 0.51 on 28 April, and kept-maintained high CE318 AODAOD to a value of 0.54 on 1 May, after that-which it decreased to 0.34 on 2 May. NAM_CO also showed the-an increase of CE318 AODAOD at-during the first two days of the period, but decreased after 29 April. QOMS_CAM showed a slight increase of-in CE318 AODAOD from 27 April to 40-30 April, which was later than those of the other two sites. Combining the EAE on these days, fine mode aerosol was brought in-to Lhasa and NAM_CO during 27-29 April, and then coarse aerosol began to occurred on 30 April, and even became the dominant aerosol in the following several days. The fine aerosol at the QOMS_CAM site kept-were maintained for an extra-additional day than-after those at the two sites, and then the coarse aerosol increased.

The GEOS-Chem model simulation also supported the above results. Figure 14Figure-13

shows the comparison between the ~~GEOS-Chem model simulated AOD~~ Model AOD ($0.5^\circ \times 0.667^\circ$) and ~~CE318-observed CE318~~ AOD at 550 nm and the ratios of the model simulated aerosol types (dust, both organic carbon (OC) and black carbon (BC) aerosol) to the total ~~Model AOD~~ AOD during this case period at the three sites. The evaluation results showed that the model underestimated the daily AOD at the three sites during ~~the this~~ period, with negative mean biases from -0.28 to -0.08. However, the ~~Model AOD~~ model AOD was relatively high correlated with the ~~CE318-CE318~~ AOD at 550 nm, with the ~~correlation coefficient (R)~~ values of 0.61 at Lhasa, 0.89 at NAM_CO and 0.86 at QOMS_CAS. These R values were higher than the model evaluation in South China and the Indo-China Plain (~0.5) (Zhu et al., 2017). Thus, ~~AOD-the~~ variation trend from Model AOD ~~the model simulation was in good agreement~~ agreed well with that measured by the CE318 instruments during these days. During the first 4 days of the case period (27 April to 30 April), the ratios of different aerosols to ~~the total Model AOD~~ AOD showed that the sum of OC and BC aerosols ~~was were~~ higher than those of dust aerosol at all ~~the~~ three sites. Besides, the sums of OC and BC at Lhasa and QOMS_CAS ~~was were~~ higher than that of NAM_CO. These indicated that the smoke aerosol affected the three sites more severely than dust during the first 4 days and Lhasa and QOMS_CAS sites were nearer to smoke sources than NAM_CO. After 30 April, the sum of BC and OC ~~was~~ decreased while dust increased, and the increase of dust at the three sites was NAM_CO > Lhasa > QOMS_CAS. Therefore, the major aerosol source was changed and the NAM_CO site was closer to dust source after ~~40-30~~ April. This phenomenon had continued to 2 May at NAM_CO and Lhasa, and 1 May at QOMS_CAS. ~~At In~~ In the last one or two days, the dust decreased while the smoke obviously increased ~~obviously~~, which could cause the mixture of ~~this~~ these two aerosols.

Then, how ~~is was~~ is the spatial aerosol loading around the TP and the vertical feature of aerosol transported to the TP? ~~Figure 15~~ Figure 14 shows ~~MODIS C6-the MODIS~~ MODIS AOD-at 550nm and 72-~~hour~~ hour back trajectories at Lhasa (the first row), the CALIOP-derived vertical profile of total attenuated backscatter at 532 nm (the second row), and the vertical feature mask of aerosol (the third row) on ~~28 April-28~~ 1 May-1, and ~~3 May-3~~ 3 May-3 during ~~this-the case study~~ period. The ~~MODIS~~ MODIS AOD showed high values in the south (South Asia) and north (Taklimakan Desert) on the three days. The ~~H~~ high values in South Asia ~~was were~~ were caused by anthropogenic aerosols (such as biomass burning) or dust polluted by anthropogenic aerosols, while the high MODIS AOD in the Taklimakan Desert ~~was~~ resulted from ~~the~~ dust. The values and areas of the high MODIS AOD in South Asia and Taklimakan Desert on ~~1 May 1~~ 1 May 1 and ~~3 May 3~~ 3 May 3 were higher and larger than ~~that those~~ those on April 28. The back-~~trajectories~~ trajectories ended at Lhasa on the three days were different. On 28 April, the air flows ~~were~~ were originated from the southwest (South Asia region). However, the air masses on 1 and 3 May were from the northwest (Taklimakan Desert).

The CALIPSO ground tracks across the TP and through South Asia and the Taklimakan Desert were chosen to show the aerosol transport to the TP sites. On 28 April, the ~~level-Level-1~~ level-Level-1 attenuated backscatter at 532 nm derived from CALIOP (the second row) showed apparent aerosol layers in the ~~S~~ southern area (Bhutan and northeast India) and this aerosol layer even ~~lifted-extended~~ lifted-extended to an altitude of ~10km ~~altitude in the sky~~ altitude in the sky over the TP along the southern slope of the TP. On 1 May, the CALIOP attenuated backscatter not only showed the deep aerosol layers in south of the TP but also showed stronger aerosol layers ~~in the north of~~ the TP (Taklimakan Desert area). Besides, the north

aerosol layers also climbed into the air over the TP, but not as high as the southern aerosol layer. On 3 May, there were also aerosol layers ~~on~~ in the south and north of the TP and ~~they that both~~ both transported to above the TP ~~overhead~~, but the aerosol loading over the TP was lower than that on 28 April and 1 May (the values of attenuated backscatter on 3 May was lower), which ~~caused~~ corresponds to the lower CE318 AOD ~~observed by CE318 at the three TP sites (Figure 12)~~ on this day ~~was lower than those on~~ 28 April and 1 May at the three TP sites (Figure 13).

The vertical feature mask of the aerosol from CALIOP (the third row) ~~shows~~ showed the aerosol types on the three days. On 28 April, the aerosol layer in the north (~~about ~~~ 35°N) and above the TP was mainly the smoke aerosol and was even higher than 10 km. The back trajectories ended at Lhasa also showed that the southern airflow brought the smoke aerosol and polluted dust from South Asia to the ~~center~~ centre of the TP. On 1 May, the aerosol layer ~~in on the~~ southern slope of the TP was also ~~the~~ smoke aerosol and polluted dust, while the aerosol layers in the northern ~~of~~ TP and above the TP ~~overhead~~ were almost all dust aerosol, which could be explained by the northwest airflows carrying the dust aerosol from the Taklimakan Desert. which These may be the result of the lower EAE values at Lhasa and NAM_CO than that at QOMS_CAM (~~Figure 13~~ Figure 12). ~~After two days mixing, On 3 May,~~ the aerosol type above the central TP and the southern TP ~~on 3 May~~ has been ~~was~~ occupied by ~~the~~ polluted dust aerosol, and the EAE at NAM_CO and QOMS_CAM also showed a little slight increase on 3 May. These results agree with the aerosol simulation ~~of from~~ GEOS-Chem. Jia et al. (2015) has shown that the dust from India polluted by anthropogenic aerosols can be transported to the TP, but the back trajectories on 1 and 3 May illustrated that the airflows that ended at Lhasa were from the north or northwest rather than the south, indicating that the polluted dust over the TP on 3 May was more likely the mixing result of dust and smoke aerosol. In addition, the lengths of the back trajectories (especially the back trajectories at 10 m and 500 m above ground level) on 1 May showed that the airflows moved slowly, which allowed the possibility of aerosol mixture over the TP. The observations and model simulations illustrated a the following scene: ~~firstly,~~ the smoke aerosol in South Asia was lifted up to 10 km, ~~contaminated~~ contaminating the TP sites, and transported to the centre of the TP; then, the dust from the Taklimakan Desert could climb the north slope of the TP and be transported to the TP; finally, the dust and smoke aerosol over the TP were mixed ~~at last~~. This case of aerosol pollution shows that the anthropogenic aerosols (mainly smoke) smoke in South Asia and Dust dust in the Taklimakan Desert could be transported to the center centre of the TP and they both even can cause ~~the~~ mixed aerosol pollution above the TP. The past cases ~~studies~~ of aerosol transport to the TP are almost individual dust or smoke aerosol, while this case of aerosol pollution over the TP ~~has shown~~ showed the mixing pollution during the last two days of the case period.

6. Conclusion

The long-term ~~temporal-spatial~~ spatiotemporal variations ~~of in the~~ aerosol optical properties and the impacts of the aerosol long-range aerosol transport ~~impact over~~ the TP were ~~analyzed~~ analysed by using a combination of ground-based and satellite remote sensing aerosol products as well as model simulations. The major conclusions are drawn as follows:

- (1) The annual CE318 AOD at most TP sites showed increasing trends (0–0.013/year) during the past decade: 0.001±0.003/year at Lhasa, 0.013±0.003/year at Mt_WLG, 0.002±0.002/year at NAM_CO, and 0.000±0.002/year at QOMS_CAS. Most sites showed the iIncreaseding

- tendency tendencies of in the annual-averaged EAE, except for Mt_WLG were also found at most TP sites with a large decreasing trend of 0.318/year. Spatially, the MODIS AOD showed negative trends in the northwest edge closed to the Taklimakan Desert and the east of Qaidam Basin and slightly positive trends in most of the other areas of the TP.
- (2) The values of EAE with AOD>0.4 at five TP ground stations showed two centers of ~0.1 and ~1.5. The EAE and size distribution during the aerosol polluted day (CE318 AOD at 440 nm > 0.4) at the TP showed the different aerosol type pollution in the five sites: dust dominant in Lhasa, Mt_WLG and Muztagh and fine mode aerosol pollution dominant at NAM_CO and QOMS_CAS. The back-trajectories on polluted days indicated the dust aerosol mainly come from the Taklimakan Desert and fine mode aerosol was mainly transported from South Asia. Different aerosol types and sources contributed to the high aerosol loading at the five sites: dust was dominant in Lhasa, Mt_WLG and Muztagh with sources from the Taklimakan Desert, but fine aerosol pollution was dominant at NAM_CO and QOMS_CAS with the transport from South Asia.
- (3) A case of smoke followed by dust pollution at Lhasa, NAM_CO and QOMS_CAS during 28 April – 3 May 2016 was analyzed: showed that firstly, the smoke aerosol in South Asia was first uplifted up to 10 km and transported to the center centre of TP; then Then, the dust from the Taklimakan Desert could climb the northern slope of the TP and be transported to the TP, allowing the dust and smoke aerosol over the TP were to mixed at last.

There are some limitations in this study. First, ground-based remote sensing and MODIS MODIS AOD products may have had missing data due to missed conditions interfered with clouds interference. Second, only half of a year of observations at the Muztagh_Ata station may not be sufficient to fully reveal pollution days in the northwest TP region, which will could have affected the statistics to some extent. More long-term in situ observations are needed in the TP. However, due to the remoteness and challenging weather conditions over the plateau, maintaining long-term in situ observation stations over the TP in long-term is very difficult. The numerical model simulation is more practically feasible to study the aerosol properties over the TP, but the model accuracy is far from being ideal over the TP. Thus, long-term numerical model simulation coupling coupled with satellite observations and intensive short-term field campaigns should be used to analyze-analyse the aerosol properties over the TP in the future.

Data availability:

The four sites (Mt_WLG, Muztagh_Ata, NAM_CO and QOMS_CAS) data are available from AERONET website (<https://aeronet.gsfc.nasa.gov/>). The dataset of Lhasa used in the study can be requested by contacting the corresponding author. The MODIS aerosol products are available from <http://ladsweb.nascom.nasa.gov>. The HYSPLIT model and meteorological fields' data can be from <https://www.arl.noaa.gov/hysplit/>. The CALIPSO data are from <https://eosweb.larc.nasa.gov>. GEOS-Chem model code and share data can be obtained from <http://wiki.seas.harvard.edu/geos-chem>.

Competing interests.

The authors declare that they have no conflict of interest.

1 Author contribution:

2 All authors help to shape the ideas and review this manuscript. JZ, XX and HC designed, and
3 wrote the manuscript; JZ, XX, HC, JW help to analyze the data; HC, XZ, SK and ZC carried out
4 the sunphotometer observations; JW, ZC, SK, TZ, XY, and YZ provided constructive comments on
5 this study.

6 7 **Acknowledgments**

8 This research was supported by the National Science Fund for Distinguished Young Scholars
9 (41825011), the National Key R & D Program Pilot Projects of China (2016YFA0601901 and
10 2016YFC0203304), the National Natural Science Foundation of China (41761144056), the
11 Strategic Priority Research Program of Chinese Academy of Sciences (XDA20040500), the Natural
12 Science Foundation of Jiangsu Province (BK20170943), the Open fund by the Key Laboratory for
13 Middle Atmosphere and Global Environment Observation (LAGEO) / Institute of Atmospheric
14 Physics, and LAC/CMA (2018B02).

References

- Ångström, A.: On the atmospheric transmission of Sun radiation and on dust in the air, Geografiska Annaler, 11, 156-166, <https://doi.org/10.1080/20014422.1929.11880498>, 1929.
- Bey, I., Jacob, D. J., Yantosca, R. M., Logan, J. A., Field, B. D., Fiore, A. M., Li, Q., Liu, H. Y., Mickley, L. J., and Schultz, M. G.: Global modeling of tropospheric chemistry with assimilated meteorology: Model description and evaluation, *Journal of Geophysical Research: Atmospheres*, 106, 23073-23095, <https://doi.org/10.1029/2001jd000807>, 2001.
- Bilal, M., Nazeer, M., Qiu, Z., Ding, X., and Wei, J.: Global Validation of MODIS C6 and C6.1 Merged Aerosol Products over Diverse Vegetated Surfaces, *Remote Sens-Basel*, 10, 475, <https://doi.org/10.3390/rs10030475>, 2018.
- Bilal, M., and Qiu, Z.: Evaluation of Modis C6 Combined Aerosol Product at Global Scale, IGARSS 2018 - 2018 IEEE International Geoscience and Remote Sensing Symposium, 2018, 9126-9129.
- Bilal, M., Nazeer, M., Nichol, J., Qiu, Z., Wang, L., Bleiweiss, M. P., Shen, X., Campbell, J. R., and Lolli, S.: Evaluation of Terra-MODIS C6 and C6.1 Aerosol Products against Beijing, XiangHe, and Xinglong AERONET Sites in China during 2004-2014, Remote Sens-Basel, 11, 486, <https://doi.org/doi:10.3390/rs11050486>, 2019.
- Che, H., Zhang, X. Y., Xia, X., Goloub, P., Holben, B., Zhao, H., Wang, Y., Zhang, X. C., Wang, H., Blarel, L., Damiri, B., Zhang, R., Deng, X., Ma, Y., Wang, T., Geng, F., Qi, B., Zhu, J., Yu, J., Chen, Q., and Shi, G.: Ground-based aerosol climatology of China: aerosol optical depths from the China Aerosol Remote Sensing Network (CARSNET) 2002–2013, *Atmospheric Chemistry and Physics*, 15, 7619-7652, <https://doi.org/10.5194/acp-15-7619-2015>, 2015.
- Che, H. Z., Wang, Y. Q., and Sun, J. Y.: Aerosol optical properties at Mt. Waliguan Observatory, China, Atmospheric Environment, 45, 6004-6009, <https://doi.org/10.1016/j.atmosenv.2011.07.050>, 2011.
- Chen, J., Xin, J., An, J., Wang, Y., Liu, Z., Chao, N., and Meng, Z.: Observation of aerosol optical properties and particulate pollution at background station in the Pearl River Delta region, Atmospheric Research, 143, 216-227, <https://doi.org/10.1016/j.atmosres.2014.02.011>, 2014.
- Cong, Z., Kang, S., Liu, X., and Wang, G.: Elemental composition of aerosol in the Nam Co region, Tibetan Plateau, during summer monsoon season, *Atmospheric Environment*, 41, 1180-1187, <https://doi.org/10.1016/j.atmosenv.2006.09.046>, 2007.
- Cong, Z., Kang, S., Smirnov, A., and Holben, B.: Aerosol optical properties at Nam Co, a remote site in central Tibetan Plateau, Atmospheric Research, 92, 42-48, <https://doi.org/10.1016/j.atmosres.2008.08.005>, 2009.
- Draxler, R. R., and Hess, G. D.: An overview of the HYSPLIT-4 Modelling system for trajectories, dispersion and deposition, *Australian Meteorological Magazine*, 47, 295-308, 1998.
- Du, W., Sun, Y. L., Xu, Y. S., Jiang, Q., Wang, Q. Q., Yang, W., Wang, F., Bai, Z. P., Zhao, X. D., and Yang, Y. C.: Chemical characterization of submicron aerosol and particle growth events at a national background site (3295 m a.s.l.) on the Tibetan Plateau, *Atmospheric Chemistry and Physics*, 15, 10811-10824, <https://doi.org/10.5194/acp-15-10811-2015>, 2015.
- Dubovik, O., and King, M. D.: A flexible inversion algorithm for retrieval of aerosol optical properties from Sun and sky radiance measurements, Journal of Geophysical Research: Atmospheres, 105, 20673-20696, <https://doi.org/10.1029/2000jd900282>, 2000.
- Dubovik, O., Holben, B., Eck, T. F., Smirnov, A., Kaufman, Y. J., King, M. D., Tanré, D., and

- 1 Slutsker, I.: Variability of Absorption and Optical Properties of Key Aerosol Types Observed
2 in Worldwide Locations, *Journal of the Atmospheric Sciences*, 59, 590-608,
3 [https://doi.org/10.1175/1520-0469\(2002\)059<0590:voaaop>2.0.co;2](https://doi.org/10.1175/1520-0469(2002)059<0590:voaaop>2.0.co;2), 2002.
- 4 Dubovik, O., Sinyuk, A., Lapyonok, T., Holben, B. N., Mishchenko, M., Yang, P., Eck, T. F., Volten,
5 H., Munoz, O., Veihelmann, B., van der Zande, W. J., Leon, J. F., Sorokin, M., and Slutsker, I.:
6 Application of spheroid models to account for aerosol particle nonsphericity in remote sensing
7 of desert dust, *J Geophys Res-Atmos*, 111, D11208.11201-D11208.11234,
8 <https://doi.org/10.1029/2005jd006619>, 2006.
- 9 Eck, T. F., Holben, B. N., Reid, J. S., Dubovik, O., Smirnov, A., O'Neill, N. T., Slutsker, I., and
10 Kinne, S.: wavelength dependence of the optical depth of biomass burning, urban, and desert
11 dust aerosols, *Journal of Geophysical Research*, 104, 31,333-331,349,
12 <https://doi.org/10.1029/1999JD900923>, 1999.
- 13 Eck, T. F., Holben, B. N., Sinyuk, A., Pinker, R. T., Goloub, P., Chen, H., Chatenet, B., Li, Z., Singh,
14 R. P., Tripathi, S. N., Reid, J. S., Giles, D. M., Dubovik, O., O'Neill, N. T., Smirnov, A., Wang,
15 P., and Xia, X.: Climatological aspects of the optical properties of fine/coarse mode aerosol
16 mixtures, *J Geophys Res-Atmos*, 115, <https://doi.org/10.1029/2010jd014002>, 2010.
- 17 Fan, X., Chen, H., Goloub, P., Xia, X., Zhang, W., and Chatenet, B.: Analysis of column-integrated
18 aerosol optical thickness in Beijing from AERONET observations, *China Particuology*, 4, 330-
19 335, [https://doi.org/10.1016/S1672-2515\(07\)60285-1](https://doi.org/10.1016/S1672-2515(07)60285-1), 2006.
- 20 Giles, D. M., Holben, B. N., Eck, T. F., Sinyuk, A., Smirnov, A., Slutsker, I., Dickerson, R. R.,
21 Thompson, A. M., and Schafer, J. S.: An analysis of AERONET aerosol absorption properties
22 and classifications representative of aerosol source regions, *J Geophys Res-Atmos*, 117, 127-
23 135, <https://doi.org/10.1029/2012JD018127>, 2012.
- 24 Giles, D. M., Sinyuk, A., Sorokin, M. G., Schafer, J. S., Smirnov, A., Slutsker, I., Eck, T. F., Holben,
25 B. N., Lewis, J. R., Campbell, J. R., Welton, E. J., Korkin, S. V., and Lyapustin, A. I.:
26 Advancements in the Aerosol Robotic Network (AERONET) Version 3 database – automated
27 near-real-time quality control algorithm with improved cloud screening for Sun photometer
28 aerosol optical depth (AOD) measurements, *Atmos Meas Tech*, 12, 169-209,
29 <https://doi.org/10.5194/amt-12-169-2019>, 2019.
- 30 Heald, C. L., Ridley, D. A., Kroll, J. H., Barrett, S. R. H., Cady-Pereira, K. E., Alvarado, M. J., and
31 Holmes, C. D.: Contrasting the direct radiative effect and direct radiative forcing of aerosols,
32 *Atmospheric Chemistry and Physics*, 14, 5513-5527, [https://doi.org/10.5194/acp-14-5513-](https://doi.org/10.5194/acp-14-5513-2014)
33 [2014](https://doi.org/10.5194/acp-14-5513-2014), 2014.
- 34 Huang, J., Minnis, P., Yi, Y., Tang, Q., Wang, X., Hu, Y., Liu, Z., Ayers, K., Trepte, C., and Winker,
35 D.: Summer dust aerosols detected from CALIPSO over the Tibetan Plateau, *Geophys Res Lett*,
36 34, 529-538, <https://doi.org/10.1029/2007gl029938>, 2007.
- 37 Jia, R., Liu, Y., Chen, B., Zhang, Z., and Huang, J.: Source and transportation of summer dust over
38 the Tibetan Plateau, *Atmospheric Environment*, 123, 210-219,
39 <https://doi.org/10.1016/j.atmosenv.2015.10.038>, 2015.
- 40 Kopacz, M., Mauzerall, D., Wang, J., Leibensperger, E., Henze, D., and Singh, K.: Origin and
41 radiative forcing of black carbon transported to the Himalayas and Tibetan Plateau,
42 *Atmospheric Chemistry and Physics*, 11, 2837-2852, [https://doi.org/10.5194/acp-11-2837-](https://doi.org/10.5194/acp-11-2837-2011)
43 [2011](https://doi.org/10.5194/acp-11-2837-2011), 2011.
- 44 Kumar, A., Singh, N., Anshumali, and Solanki, R.: Evaluation and utilization of MODIS and

- CALIPSO aerosol retrievals over a complex terrain in Himalaya, Remote Sensing of Environment, 206, 139-155, <https://doi.org/10.1016/j.rse.2017.12.019>, 2018.
- Lau, K. M., Kim, M. K., and Kim, K. M.: Asian summer monsoon anomalies induced by aerosol direct forcing: the role of the Tibetan Plateau, *Clim Dynam*, 26, 855-864, <https://doi.org/10.1007/s00382-006-0114-z>, 2006.
- Lee, W.-S., Bhawar, R. L., Kim, M.-K., and Sang, J.: Study of aerosol effect on accelerated snow melting over the Tibetan Plateau during boreal spring, *Atmospheric Environment*, 75, 113-122, <https://doi.org/10.1016/j.atmosenv.2013.04.004>, 2013.
- Levy, R. C., Mattoo, S., Munchak, L. A., Remer, L. A., Sayer, A. M., Patadia, F., and Hsu, N. C.: The Collection 6 MODIS aerosol products over land and ocean, *Atmos Meas Tech*, 6, 2989-3034, <https://doi.org/10.5194/amt-6-2989-2013>, 2013.
- Li, J., Huang, J., Stamnes, K., Wang, T., Lv, Q., and Jin, H.: A global survey of cloud overlap based on CALIPSO and CloudSat measurements, *Atmospheric Chemistry and Physics*, 15, 519-536, <https://doi.org/10.5194/acp-15-519-2015>, 2015.
- Li, J., Lv, Q., Zhang, M., Wang, T., Kawamoto, K., Chen, S., and Zhang, B.: Effects of atmospheric dynamics and aerosols on the fraction of supercooled water clouds, *Atmospheric Chemistry and Physics*, 17, 1847-1863, <https://doi.org/10.5194/acp-17-1847-2017>, 2017.
- Li, J., Jian, B., Huang, J., Hu, Y., Zhao, C., Kawamoto, K., Liao, S., and Wu, M.: Long-term variation of cloud droplet number concentrations from space-based Lidar, *Remote Sensing of Environment*, 213, 144-161, <https://doi.org/10.1016/j.rse.2018.05.011>, 2018.
- Li, M., Zhang, Q., Streets, D. G., He, K. B., Cheng, Y. F., Emmons, L. K., Huo, H., Kang, S. C., Lu, Z., Shao, M., Su, H., Yu, X., and Zhang, Y.: Mapping Asian anthropogenic emissions of non-methane volatile organic compounds to multiple chemical mechanisms, *Atmospheric Chemistry and Physics*, 14, 5617-5638, <https://doi.org/10.5194/acp-14-5617-2014>, 2014.
- Liu, Y., Sato, Y., Jia, R., Xie, Y., Huang, J., and Nakajima, T.: Modeling study on the transport of summer dust and anthropogenic aerosols over the Tibetan Plateau, *Atmospheric Chemistry and Physics*, 15, 12581-12594, <https://doi.org/10.5194/acp-15-12581-2015>, 2015.
- Liu, Z., Liu, D., Huang, J., Vaughan, M., Uno, I., Sugimoto, N., Kittaka, C., Trepte, C., Wang, Z., Hostetler, C., and Winker, D.: Airborne dust distributions over the Tibetan Plateau and surrounding areas derived from the first year of CALIPSO lidar observations, *Atmospheric Chemistry and Physics*, 8, 5045-5060, <https://doi.org/10.5194/acp-8-5045-2008>, 2008.
- Lu, Z., Streets, D. G., Zhang, Q., and Wang, S.: A novel back-trajectory analysis of the origin of black carbon transported to the Himalayas and Tibetan Plateau during 1996-2010, *Geophys Res Lett*, 39, n/a-n/a, <https://doi.org/10.1029/2011gl049903>, 2012.
- Ma, Y., Li, Z., Li, Z., Xie, Y., Fu, Q., Li, D., Zhang, Y., Xu, H., and Li, K.: Validation of MODIS Aerosol Optical Depth Retrieval over Mountains in Central China Based on a Sun-Sky Radiometer Site of SONET, *Remote Sens-Basel*, 8, 111, <https://doi.org/10.3390/rs8020111>, 2016.
- Martin, R. V., Jacob, D. J., Yantosca, R. M., Chin, M., and Ginoux, P.: Global and regional decreases in tropospheric oxidants from photochemical effects of aerosols, *J Geophys Res-Atmos*, 108, <https://doi.org/10.1029/2002jd002622>, 2003.
- Pan, L., Che, H., Geng, F., Xia, X., Wang, Y., Zhu, C., Chen, M., Gao, W., and Guo, J.: Aerosol optical properties based on ground measurements over the Chinese Yangtze Delta Region, Atmospheric Environment, 44, 2587-2596, <https://doi.org/10.1016/j.atmosenv.2010.04.013>,

- 2010.
- Qian, Y., Flanner, M. G., Leung, L. R., and Wang, W.: Sensitivity studies on the impacts of Tibetan Plateau snowpack pollution on the Asian hydrological cycle and monsoon climate, *Atmospheric Chemistry and Physics*, 11, 1929-1948, <https://doi.org/10.5194/acp-11-1929-2011>, 2011.
- Sayer, A. M., Munchak, L. A., Hsu, N. C., Levy, R. C., Bettenhausen, C., and Jeong, M. J.: MODIS Collection 6 aerosol products: Comparison between Aqua's e-Deep Blue, Dark Target, and "merged" data sets, and usage recommendations, *Journal of Geophysical Research: Atmospheres*, 119, 13,965-913,989, <https://doi.org/10.1002/2014jd022453>, 2014.
- Shen, R. Q., Ding, X., He, Q. F., Cong, Z. Y., Yu, Q. Q., and Wang, X. M.: Seasonal variation of secondary organic aerosol tracers in Central Tibetan Plateau, *Atmospheric Chemistry and Physics*, 15, 8781-8793, <https://doi.org/10.5194/acp-15-8781-2015>, 2015.
- Takemura, T., Nozawa, T., Emori, S., Nakajima, T. Y., and Nakajima, T.: Simulation of climate response to aerosol direct and indirect effects with aerosol transport-radiation model, *Journal of Geophysical Research*, 110, -, <https://doi.org/10.1029/2004jd005029>, 2005.
- Tobo, Y., Iwasaka, Y., Shi, G.-Y., Kim, Y.-S., Ohashi, T., Tamura, K., and Zhang, D.: Balloon-borne observations of high aerosol concentrations near the summertime tropopause over the Tibetan Plateau, *Atmospheric Research*, 84, 233-241, <https://doi.org/10.1016/j.atmosres.2006.08.003>, 2007.
- van der Werf, G. R., Randerson, J. T., Giglio, L., Collatz, G. J., Mu, M., Kasibhatla, P. S., Morton, D. C., DeFries, R. S., Jin, Y., and van Leeuwen, T. T.: Global fire emissions and the contribution of deforestation, savanna, forest, agricultural, and peat fires (1997–2009), *Atmospheric Chemistry and Physics*, 10, 11707-11735, <https://doi.org/10.5194/acp-10-11707-2010>, 2010.
- Wan, X., Kang, S., Wang, Y., Xin, J., Liu, B., Guo, Y., Wen, T., Zhang, G., and Cong, Z.: Size distribution of carbonaceous aerosols at a high-altitude site on the central Tibetan Plateau (Nam Co Station, 4730ma.s.l.), *Atmospheric Research*, 153, 155-164, <https://doi.org/10.1016/j.atmosres.2014.08.008>, 2015.
- Wang, P., Che, H. Z., Zhang, X. C., Song, Q. L., Wang, Y. Q., Zhang, Z. H., Dai, X., and Yu, D. J.: Aerosol optical properties of regional background atmosphere in Northeast China, *Atmospheric Environment*, 44, 4404-4412, <https://doi.org/10.1016/j.atmosenv.2010.07.043>, 2010.
- Wang, X., Ren, J., Gong, P., Wang, C., Xue, Y., Yao, T., and Lohmann, R.: Spatial distribution of the persistent organic pollutants across the Tibetan Plateau and its linkage with the climate systems: a 5-year air monitoring study, *Atmospheric Chemistry and Physics*, 16, 6901-6911, <https://doi.org/10.5194/acp-16-6901-2016>, 2016.
- Wang, Y. X., McElroy, M. B., Jacob, D. J., and Yantosca, R. M.: A nested grid formulation for chemical transport over Asia: Applications to CO, *Journal of Geophysical Research: Atmospheres*, 109, n/a-n/a, <https://doi.org/10.1029/2004jd005237>, 2004.
- Winker, D. M., Pelon, J., Coakley, J. A., Ackerman, S. A., Charlson, R. J., Colarco, P. R., Flamant, P., Fu, Q., Hoff, R. M., Kittaka, C., Kubar, T. L., Le Treut, H., McCormick, M. P., Megie, G., Poole, L., Powell, K., Trepte, C., Vaughan, M. A., and Wielicki, B. A.: THE CALIPSO MISSION A Global 3D View of Aerosols and Clouds, *B Am Meteorol Soc*, 91, 1211-1229, <https://doi.org/10.1175/2010bams3009.1>, 2010.
- Xia, X., Che, H., Zhu, J., Chen, H., Cong, Z., Deng, X., Fan, X., Fu, Y., Goloub, P., Jiang, H., Liu,

- Q., Mai, B., Wang, P., Wu, Y., Zhang, J., Zhang, R., and Zhang, X.: Ground-based remote sensing of aerosol climatology in China: Aerosol optical properties, direct radiative effect and its parameterization, *Atmospheric Environment*, 124, 243-251, <https://doi.org/10.1016/j.atmosenv.2015.05.071>, 2016.
- Xia, X. G., Wang, P. C., Wang, Y. S., Li, Z. Q., Xin, J. Y., Liu, J., and Chen, H. B.: Aerosol optical depth over the Tibetan Plateau and its relation to aerosols over the Taklimakan Desert, *Geophys Res Lett*, 35, 96-106, <https://doi.org/10.1029/2008gl034981>, 2008.
- Xia, X. G., Zong, X. M., Cong, Z. Y., Chen, H. B., Kang, S. C., and Wang, P. C.: Baseline continental aerosol over the central Tibetan plateau and a case study of aerosol transport from South Asia, *Atmospheric Environment*, 45, 7370-7378, <https://doi.org/10.1016/j.atmosenv.2011.07.067>, 2011.
- Xin, J. Y., Wang, Y. S., Li, Z. Q., Wang, P. C., Hao, W. M., Nordgren, B. L., Wang, S. G., Liu, G. R., Wang, L. L., Wen, T. X., Sun, Y., and Hu, B.: Aerosol optical depth (AOD) and Angstrom exponent of aerosols observed by the Chinese Sun Hazemeter Network from August 2004 to September 2005, *J Geophys Res-Atmos*, 112, 1703-1711, <https://doi.org/10.1029/2006jd007075>, 2007.
- Xing, C., Liu, C., Wang, S., Chan, K. L., Gao, Y., Huang, X., Su, W., Zhang, C., Dong, Y., Fan, G., Zhang, T., Chen, Z., Hu, Q., Su, H., Xie, Z., and Liu, J.: Observations of the vertical distributions of summertime atmospheric pollutants and the corresponding ozone production in Shanghai, China, *Atmospheric Chemistry and Physics*, 17, 14275-14289, <https://doi.org/10.5194/acp-17-14275-2017>, 2017.
- Yang, R., Wang, J., Zhang, T., and He, S.: Change in the relationship between the Australian summer monsoon circulation and boreal summer precipitation over Central China in the late 1990s, *Meteorology and Atmospheric Physics*, 131, 105-113, <https://doi.org/10.1007/s00703-017-0556-3>, 2017a.
- Yang, R. W., Tao, Y., and Cao, J.: A Mechanism for the Interannual Variation of the Early Summer East Asia-Pacific Teleconnection Wave Train, *Acta Meteorol Sin*, 24, 452-458, 2010.
- Yang, Y., Russell, L. M., Lou, S., Liao, H., Guo, J., Liu, Y., Singh, B., and Ghan, S. J.: Dust-wind interactions can intensify aerosol pollution over eastern China, *Nature communications*, 8, 15333, <https://doi.org/10.1038/ncomms15333>, 2017b.
- Zhang, B., Wang, Y., and Hao, J.: Simulating aerosol–radiation–cloud feedbacks on meteorology and air quality over eastern China under severe haze conditions in winter, *Atmospheric Chemistry and Physics*, 15, 2387-2404, <https://doi.org/10.5194/acp-15-2387-2015>, 2015.
- Zhang, N., Cao, J., Ho, K., and He, Y.: Chemical characterization of aerosol collected at Mt. Yulong in wintertime on the southeastern Tibetan Plateau, *Atmospheric Research*, 107, 76-85, <https://doi.org/10.1016/j.atmosres.2011.12.012>, 2012.
- Zhang, X. Y., Arimoto, R., Cao, J. J., An, Z. S., and Wang, D.: Atmospheric dust aerosol over the Tibetan Plateau, *Journal of Geophysical Research: Atmospheres*, 106, 18471-18476, <https://doi.org/10.1029/2000jd900672>, 2001.
- Zhao, Z., Cao, J., Shen, Z., Xu, B., Zhu, C., Chen, L. W. A., Su, X., Liu, S., Han, Y., Wang, G., and Ho, K.: Aerosol particles at a high-altitude site on the Southeast Tibetan Plateau, China: Implications for pollution transport from South Asia, *Journal of Geophysical Research: Atmospheres*, 118, 11,360-311,375, <https://doi.org/10.1002/jgrd.50599>, 2013.
- Zhu, J., Che, H., Xia, X., Chen, H., Goloub, P., and Zhang, W.: Column-integrated aerosol optical

- and physical properties at a regional background atmosphere in North China Plain, *Atmospheric Environment*, 84, 54-64, <https://doi.org/10.1016/j.atmosenv.2013.11.019>, 2014.
- Zhu, J., Xia, X., Che, H., Wang, J., Zhang, J., and Duan, Y.: Study of aerosol optical properties at Kunming in southwest China and long-range transport of biomass burning aerosols from North Burma, *Atmospheric Research*, 169, 237-247, <https://doi.org/10.1016/j.atmosres.2015.10.012>, 2016.
- Zhu, J., Xia, X., Wang, J., Zhang, J., Wiedinmyer, C., Fisher, J. A., and Keller, C. A.: Impact of Southeast Asian smoke on aerosol properties in Southwest China: First comparison of model simulations with satellite and ground observations, *Journal of Geophysical Research: Atmospheres*, 122, 3904-3919, <https://doi.org/10.1002/2016jd025793>, 2017.
- Zhuang, B. L., Wang, T. J., Liu, J., Li, S., Xie, M., Han, Y., Chen, P. L., Hu, Q. D., Yang, X. Q., Fu, C. B., and Zhu, J. L.: The surface aerosol optical properties in the urban area of Nanjing, west Yangtze River Delta, China, *Atmospheric Chemistry and Physics*, 17, 1143-1160, <https://doi.org/10.5194/acp-17-1143-2017>, 2017.
- Zhuang, B. L., Wang, T. J., Liu, J. N. E., Che, H. Z., Han, Y., Fu, Y., Li, S., Xie, M., Li, M. M., Chen, P. L., Chen, H. M., Yang, X. Q., and Sun, J. N.: The optical properties, physical properties and direct radiative forcing of urban columnar aerosols in the Yangtze River Delta, China, *Atmospheric Chemistry and Physics*, 18, 1419-1436, <https://doi.org/10.5194/acp-18-1419-2018>, 2018.

Figure captions

Figure 1. Topography of the Tibetan Plateau (TP) and the five CE318 stations located in the TP (Lhasa, Mt_WLG, Mutztagh_Ata, NAM_CO, and QOMS_CAS).~~Figure 1. Topography of Tibetan Plateau (TP) and the five CE318 stations located in TP (Lhasa, Mt_WLG, Mutztagh_Ata, NAM_CO, and QOMS_CAS).~~

Figure 2. Box plots of the monthly AOD and EAE at the five sites located on the Tibetan Plateau, i.e., Lhasa, Mt_WLG, Muztagh_Alt, NAM_CO, and QOMS_CAS. In each box, the red-line in the centre is the median and the lower and upper limits are the first and the third quartiles, respectively. The lines extending vertically from the box indicate the spread of the distribution with the length being 1.5 times the difference between the first and the third quartiles. The asterisk symbols indicate the geometric means in each month. The annual mean values and standard errors are also shown in each subgraph.~~Figure 2. Box plots of monthly AOD and EAE at the five sites located in Tibetan Plateau, i.e. Lhasa, Mt_WLG, Muztagh_Alt, NAM_CO, and QOMS_CAS. In each box, the central red-line is the median and the lower and upper limits are the first and the third quartiles, respectively. The lines extending vertically from the box indicate the spread of the distribution with the length being 1.5 times the difference between the first and the third quartiles. The asterisk symbols indicate the geometric means in each month. The annual mean values and standard errors are also shown in each subgraph.~~

Figure 3. Seasonal variation in aerosol size distribution at the five sites located in Tibetan Plateau.~~Figure 3. Seasonal variation of aerosol size distribution at the five sites located in Tibetan Plateau.~~

Figure 4. Annual averages of and trends in aerosol optical depth (AOD) and Extinction Ångstrom exponent (EAE) at four sites located in Tibetan Plateau.~~Figure 4. Annual average and the trends of aerosol optical depth (AOD) and Extinction Ångstrom exponent (EAE) at four sites located in Tibetan Plateau.~~

Figure 5. Comparisons of the 550 nm AOD measured by the CE318 instrument (CE318_AOD) over Tibetan Plateau stations with the MODIS retrieval Deep-Blue/Dark-Target combined AOD of 10 km spatial resolutions (MODIS_AOD). The statistical parameters in this figure include the number of matchup data (N), the slope and intercept at the y-axis of linear regression (read line), the mean bias (MB), root mean squared error (RMSE), correlation coefficient (R), and the percentage of data within the expected error $0.05+0.15AOD$ (%EE) which is used as the MODIS AOD expected uncertainty over land (green lines).~~Figure 5. Comparisons of AOD at 550nm measured by CE318 sunphotometer (CE318_AOD) over Tibetan Plateau stations with the MODIS retrieval Deep-Blue/Dark Target combined AOD of 10km spatial resolutions (MODIS_AOD). The statistical parameters in this figure include the number of matchup data (N), the slope and intercept at y axis of linear regression (read line), the mean bias (MB), root mean squared error (RMSE), correlation coefficient (R), and the percentage of data within the expected error $0.05+0.15AOD$ (%EE) which is used as the MODIS AOD expected uncertainty over land (green lines).~~

Figure 6. Spatial distribution of MODIS C6 AOD at 550 nm over the Tibetan Plateau (only the altitude > 3000 m) during 2006-2017. The color-filled circles are the CE318 observation AOD averages at TP sites.~~Figure 6. Spatial distribution of MODIS C6 AOD at 550nm over Tibetan Plateau~~

(only the altitude > 3000m) during 2006–2017. The circle with color filled is the CE318 observation AOD averages at TP sites.

Figure 7. The seasonal departure of MODIS AOD over the TP (altitude > 3000 m).~~Figure 7. The seasonal departure of MODIS AOD over TP (altitude > 3000m).~~

Figure 8. Trend in the MODIS AOD at 550 nm during 2006–2017.~~Figure 8. Trend of MODIS AOD at 550nm during 2006–2017.~~

Figure 9. Trends in the MODIS AOD at 550 nm during 2006–2017 in each season.~~Figure 9. Trends of MODIS AOD at 550nm during 2006–2017 in each season.~~

Figure 10. AOD vs EAE (only CE318 AOD at 440 nm > 0.4 was considered) observed by CE318 at the five sites on the Tibetan Plateau.~~Figure 10. AOD vs EAE (Only CE318 AOD at 440nm > 0.4 is considered) observed by CE318 at the five site Tibetan plateau.~~

Figure 11. Aerosol size distribution binned by CE318 AOD at the five sites on the Tibetan Plateau.~~Figure 11. Aerosol size distribution binned by CE318 AOD at the five sites in Tibetan plateau.~~

Figure 12. The back-trajectories ended at the five sites (10 m above ground level) on the TP overlaid with the mean MODIS C6 AOD at 550 nm on the aerosol pollution day observed by ground-based CE318 (CE318 AOD > 0.4). Red stands for EAE > 1.0, black for EAE < 0.5, and green for EAE within 0.5–1.0.~~Figure 12. Back trajectories ended at the five site (10 m above ground level) in TP overlaid by the mean MODIS C6 AOD at 550 nm on the aerosol pollution day observed by ground base CE318 (CE318 AOD > 0.4). Red stands for EAE > 1.0, black is EAE < 0.5, and green is for EAE within 0.5–1.0.~~

Figure 13. CE318 observed daily AOD at 440 nm and EAE during 27 April, 2016 – 3 May, 2016 at Lhasa, NAM_CO and QOMS_CAS.~~Figure 13. CE318 observed daily AOD at 440nm and EAE during April 27, 2016 – May 3, 2016 at Lhasa, NAM_CO and QOMS_CAS.~~

Figure 14. The GEOS-Chem model simulated the daily average AOD vs CE318 observed daily AOD at 550 nm, and the ratios of dust or organic carbon (OC) and black carbon (BC) aerosol to the total AOD during 27 April, 2016 – 3 May, 2016 at Lhasa, NAM_CO and QOMS_CAS. The statistical parameters used in the modal evaluation are the same as those in Figure 5.~~Figure 14. The GEOS-Chem model simulated daily average AOD vs CE318 observed daily AOD at 550nm, and the ratios of dust or organic carbon (OC) and black carbon (BC) aerosol to the total AOD during April 27, 2016 – May 3, 2016 at Lhasa, NAM_CO and QOMS_CAS. The statistical parameters used in Modal evaluation are same as Figure 5.~~

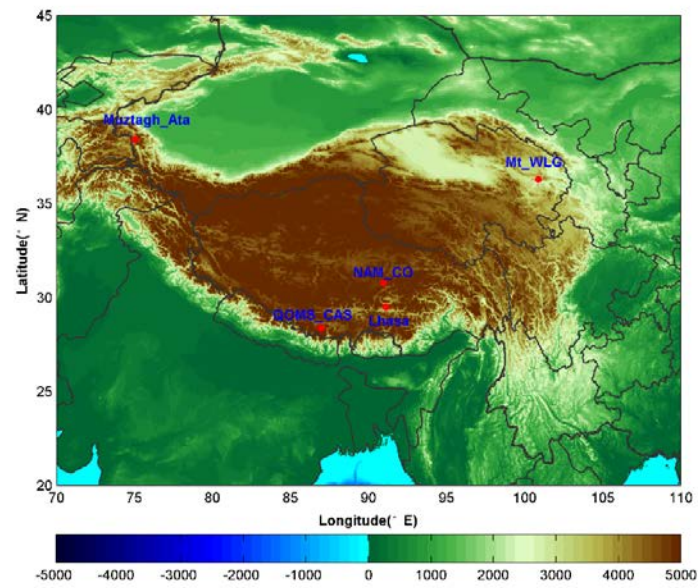
Figure 15. The MODIS C6 AOD at 550 nm and 72-hour back trajectories ended at Lhasa at three heights above the ground level (10 m in black, 500 m in red and 1000 m in blue lines) (the first row); the CALIOP-derived vertical profile of total attenuated backscatter at 532 nm (the second row); and the vertical feature mask of aerosol on 28 April, 1 May, and 3 May, 2016 over the ground track shown in the first row (green lines) (the third row).~~Figure 15. MODIS C6 AOD at 550 nm and 72h back trajectories ended at Lhasa at three heights above the ground level (10 m with black, 500 m with red and 1000 m with blue lines) (the first row), CALIOP-derived vertical profile of total~~

1 ~~attenuated backscatter at 532 nm (the second row), vertical feature mask of aerosol on April 28,~~
2 ~~May 1, and May 3, 2016 over the ground track shown in the first row (green line) (the third row).~~

3

4

1



2

3

Figure 2. Topography of the Tibetan Plateau (TP) and the five CE318 stations located in the TP (Lhasa, Mt_WLG, Mutztagh_Ata, NAM_CO, and QOMS_CAS).

4

5

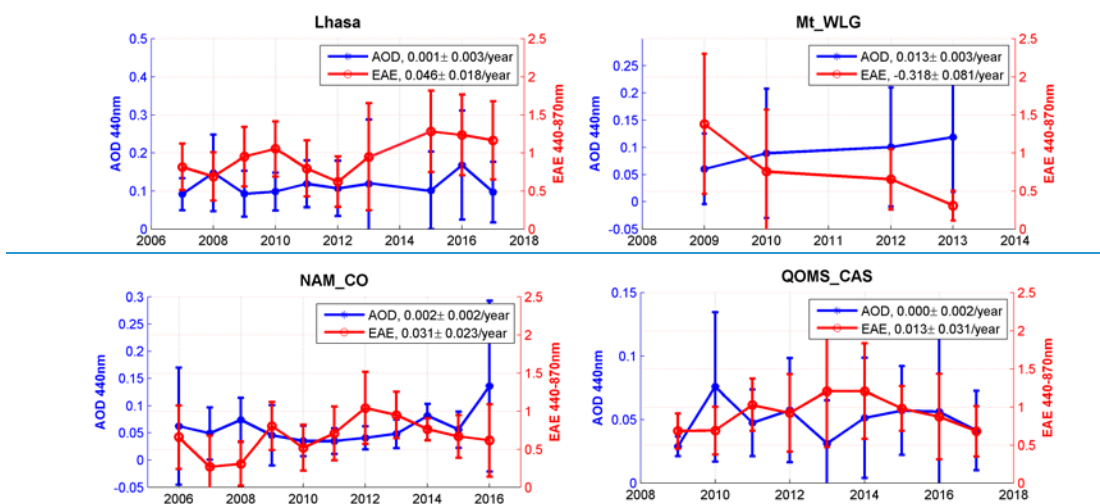


Figure 2. Annual average and the trends of aerosol optical depth (AOD) and Extinction Ångström exponent (EAE) at four sites located in Tibetan Plateau.

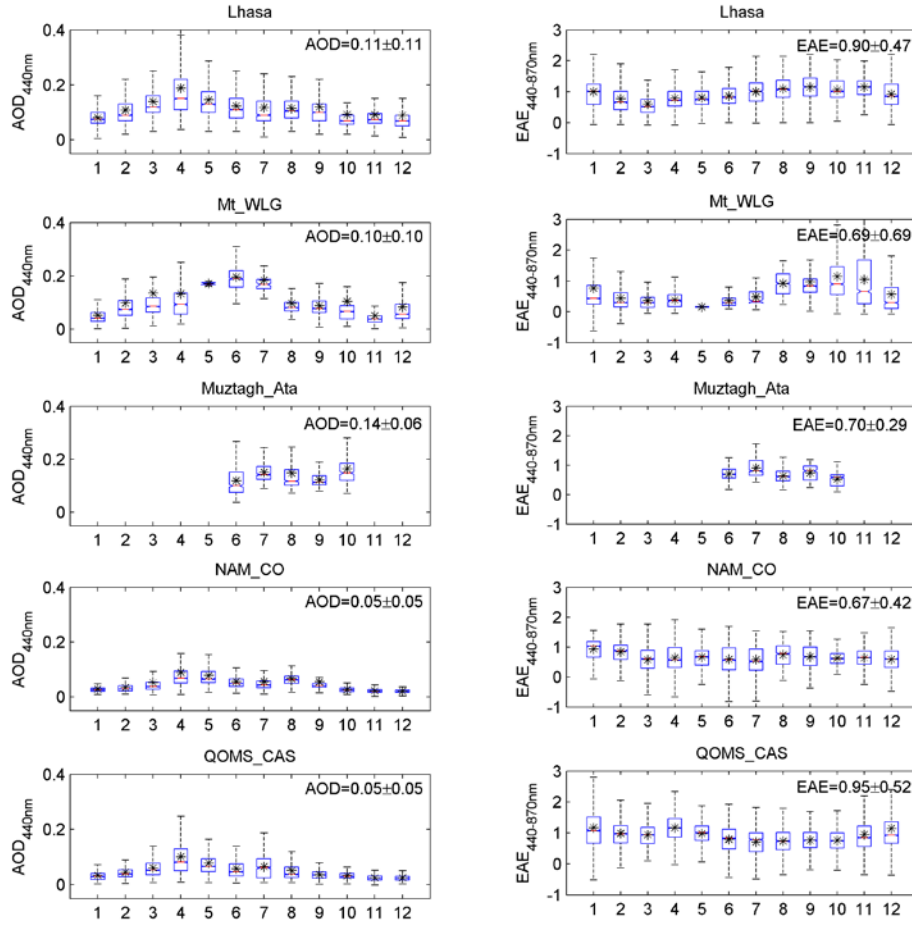


Figure 3. Box plots of the monthly AOD and EAE at the five sites located on the Tibetan Plateau, i.e., Lhasa, Mt_WLG, Muztagh_Alt, NAM_CO, and QOMS_CAS. In each box, the central-red-line in the centre is the median and the lower and upper limits are the first and the third quartiles, respectively. The lines extending vertically from the box indicate the spread of the distribution with the length being 1.5 times the difference between the first and the third quartiles. The asterisk symbols indicate the geometric means in each month. The annual mean values and standard errors are also shown in each subgraph.

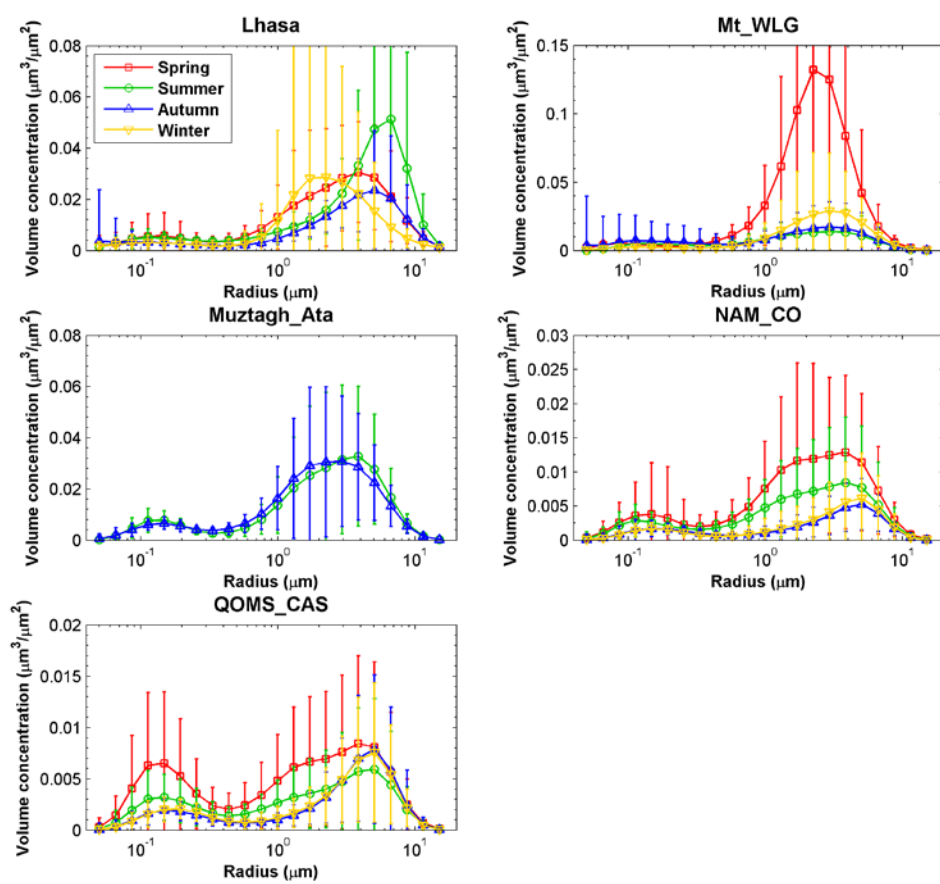


Figure 4. Seasonal variation of aerosol size distribution at the five sites located in Tibetan Plateau.

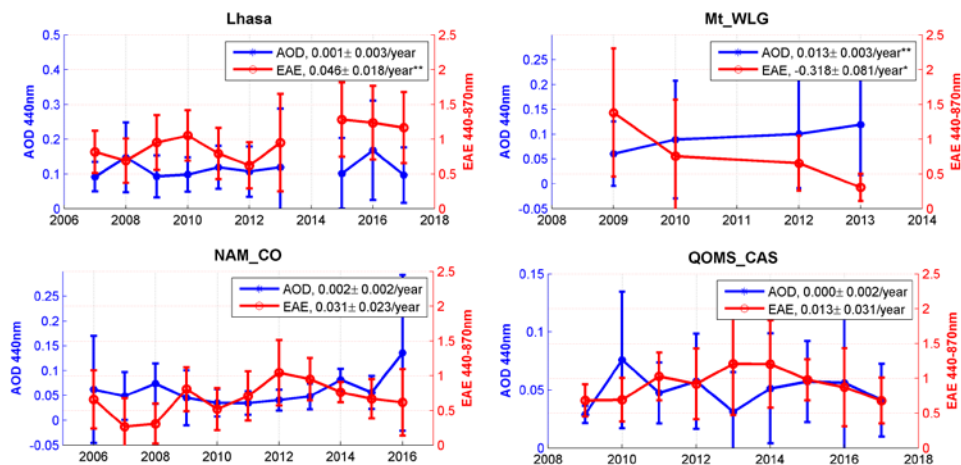
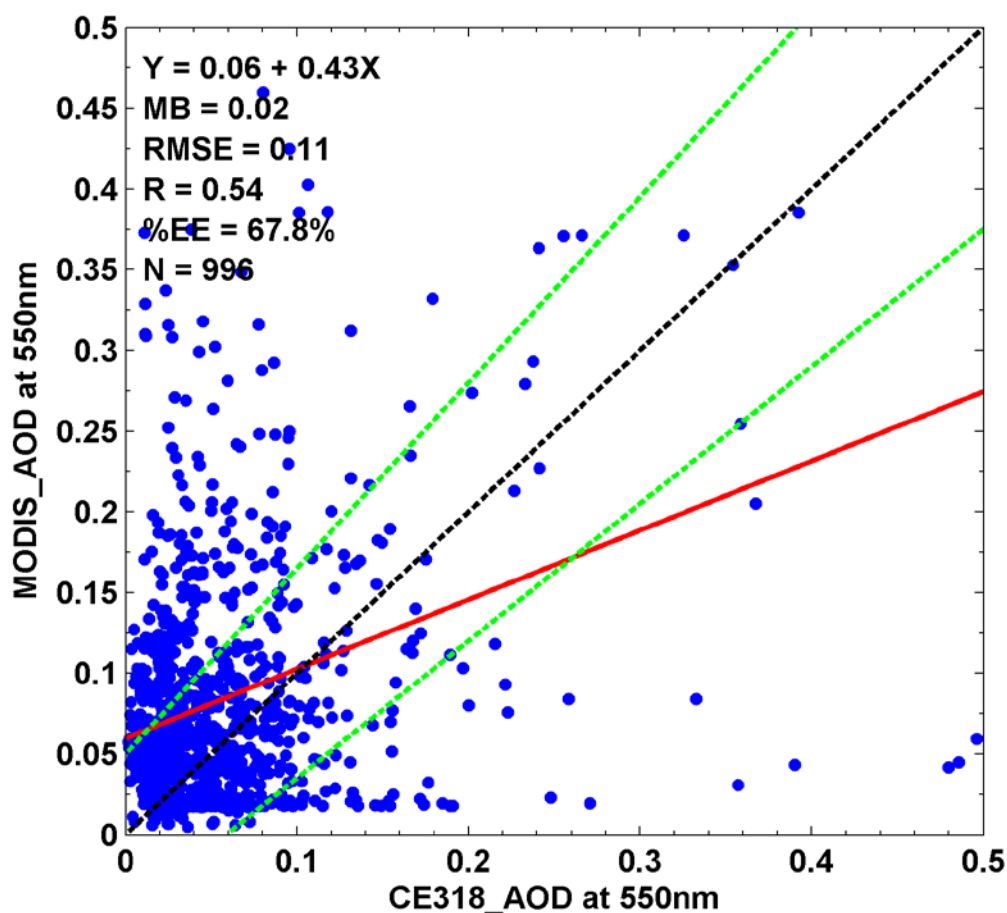


Figure 5. Annual averages of and trends in aerosol optical depth (AOD) and Extinction Ångström exponent (EAE) at four sites located in Tibetan Plateau. * stands for 90% significance, and ** represents 95% significance.

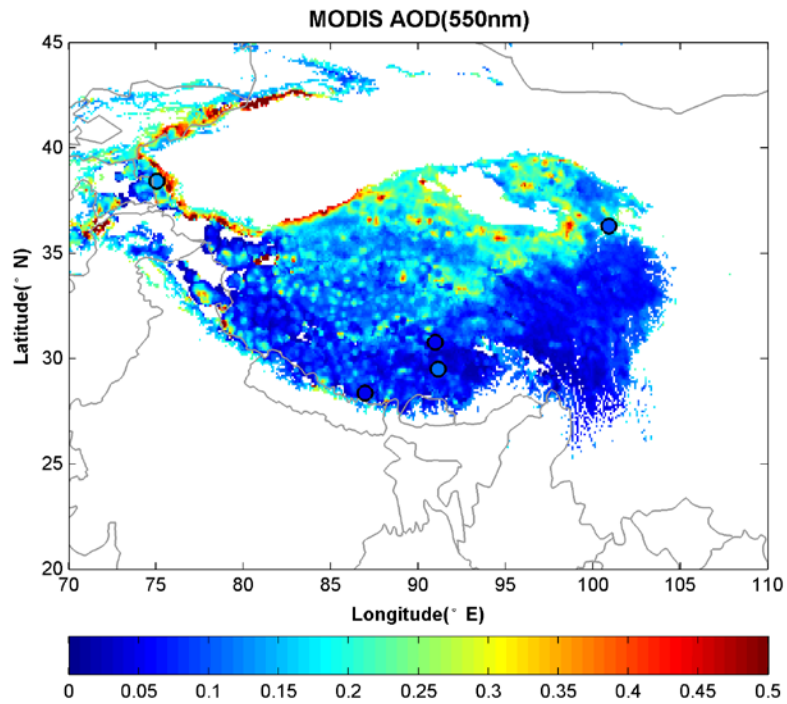
1



2

3 Figure 6. Comparisons of the 550 nm AOD measured by the CE318 instrument (CE318 AOD) over
 4 Tibetan Plateau stations with the MODIS retrieval Deep-Blue/Dark-Target combined AOD of 10 km
 5 spatial resolutions (MODIS AOD). The statistical parameters in this figure include the number of
 6 matchup data (N), the slope and intercept at the y-axis of linear regression (red line), the mean bias
 7 (MB), root mean squared error (RMSE), correlation coefficient (R), and the percentage of data within
 8 the expected error $0.05+0.15AOD$ (%EE) which is used as the MODIS AOD expected uncertainty over
 9 land (green lines).

10



1
2 Figure 7. Spatial distribution of MODIS C6 AOD at 550 nm over the Tibetan Plateau (only the altitude >
3 3000 m) during 2006-2017. The color-filled circles with color-filled is are the CE318 observation AOD
4 averages at TP sites.
5

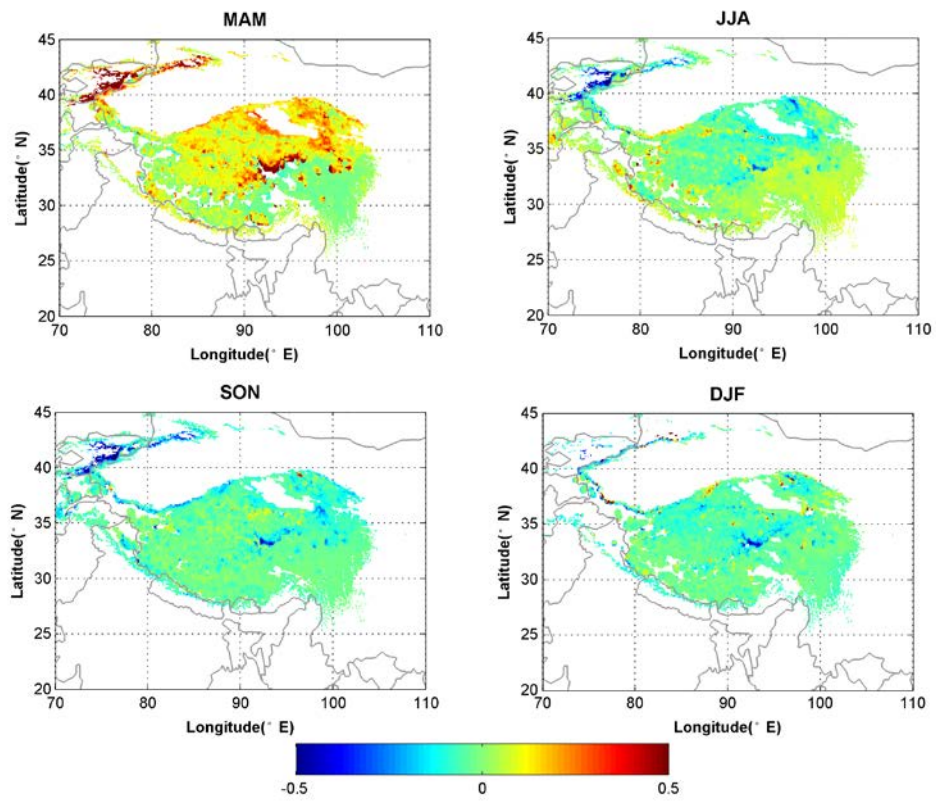


Figure 8. The seasonal departure of MODIS AOD over the TP (altitude > 3000 m).

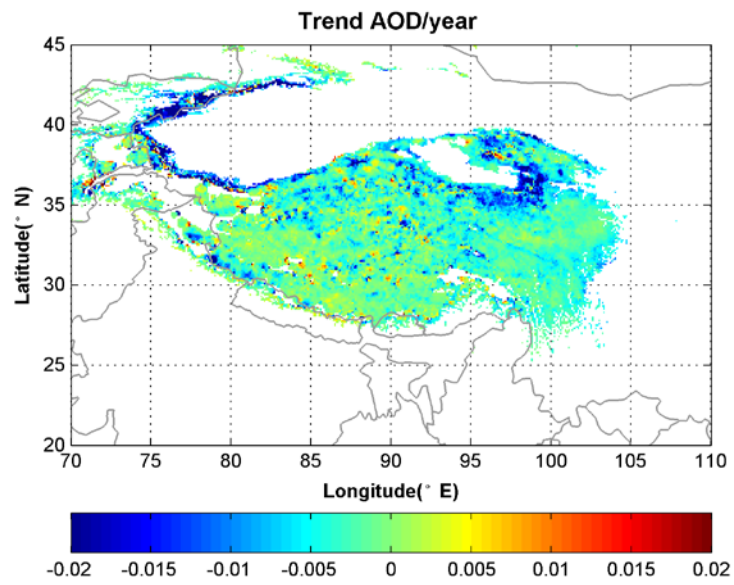


Figure 9. Trend of in the MODIS AOD at 550 nm during 2006-2017.

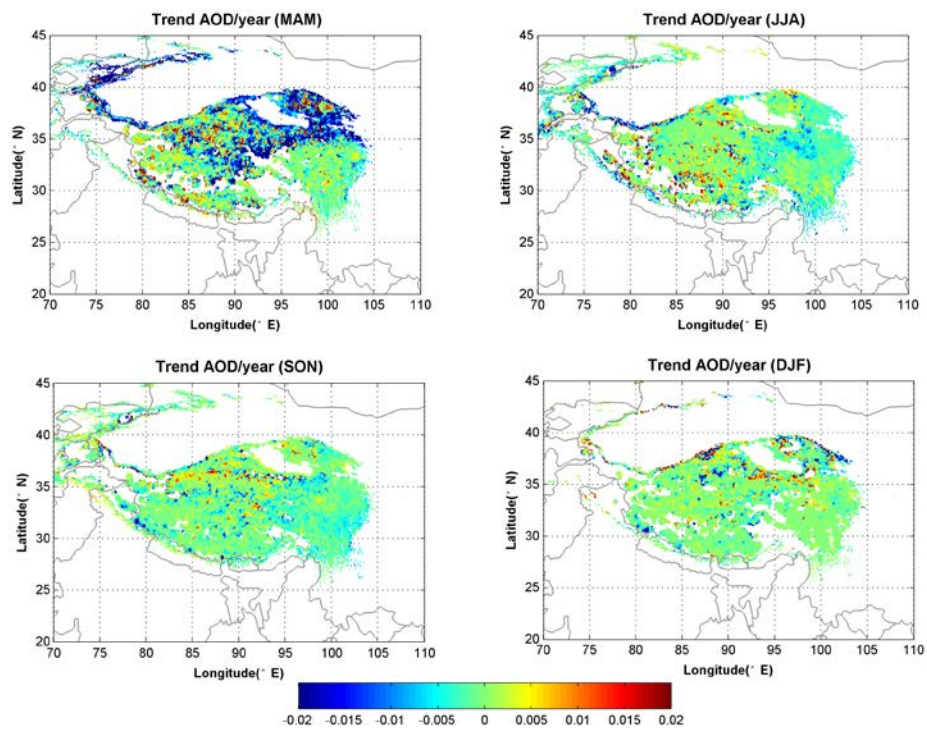


Figure 10. Trends of in the MODIS AOD at 550 nm during 2006-2017 in each season.

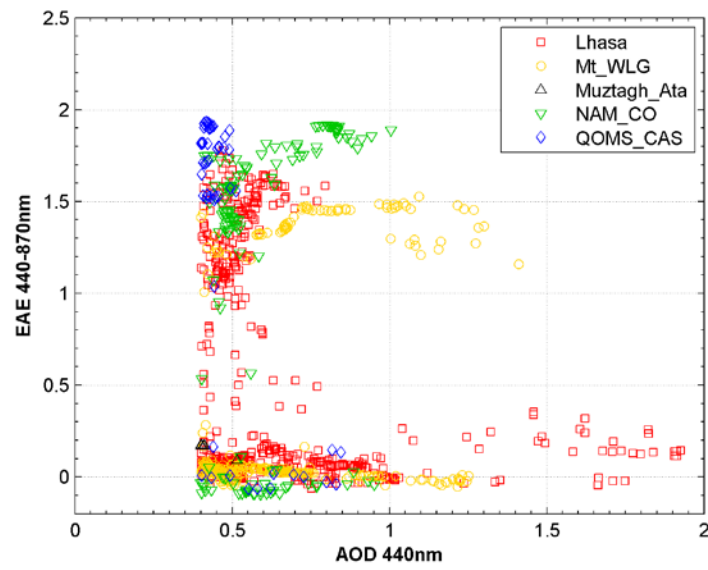


Figure 11. AOD vs EAE (Only CE318 AOD at 440_nm > 0.4 is considered) observed by CE318 at the five sites on the Tibetan plateau.

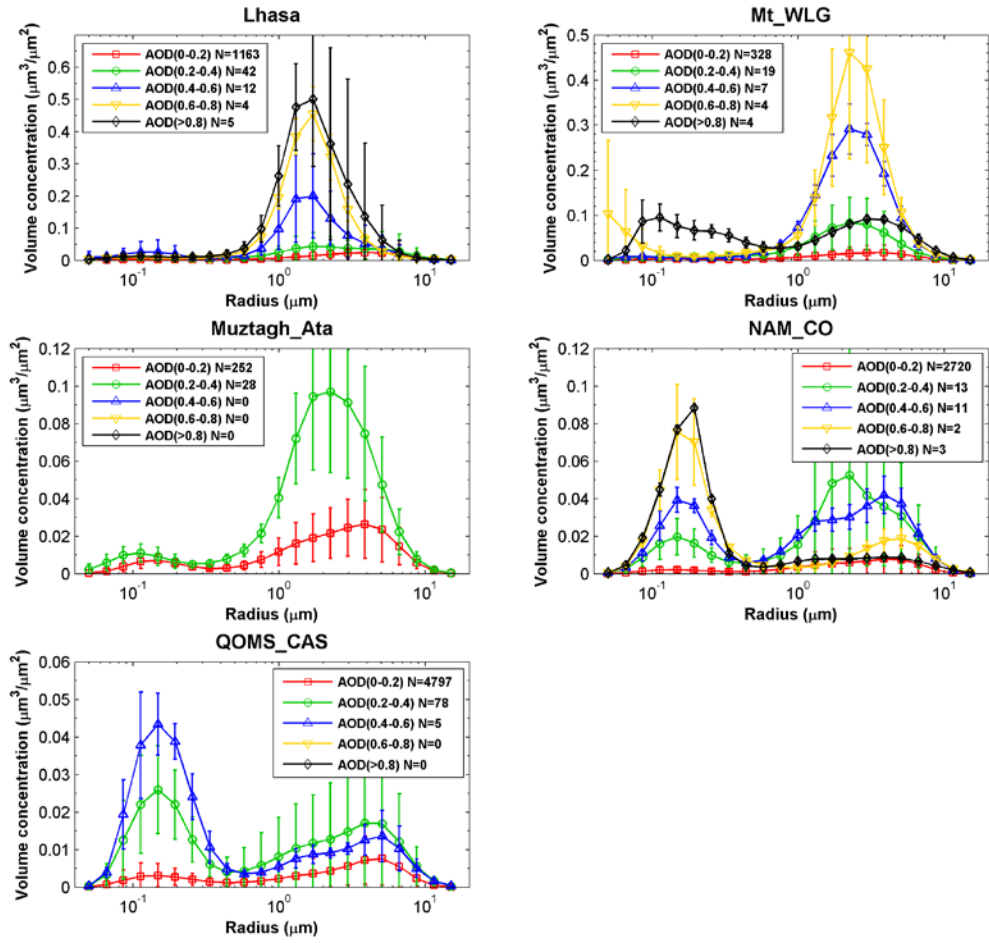


Figure 12. Aerosol size distribution binned by CE318 AOD at the five sites ~~in~~ on the Tibetan ~~plateau~~ Plateau.

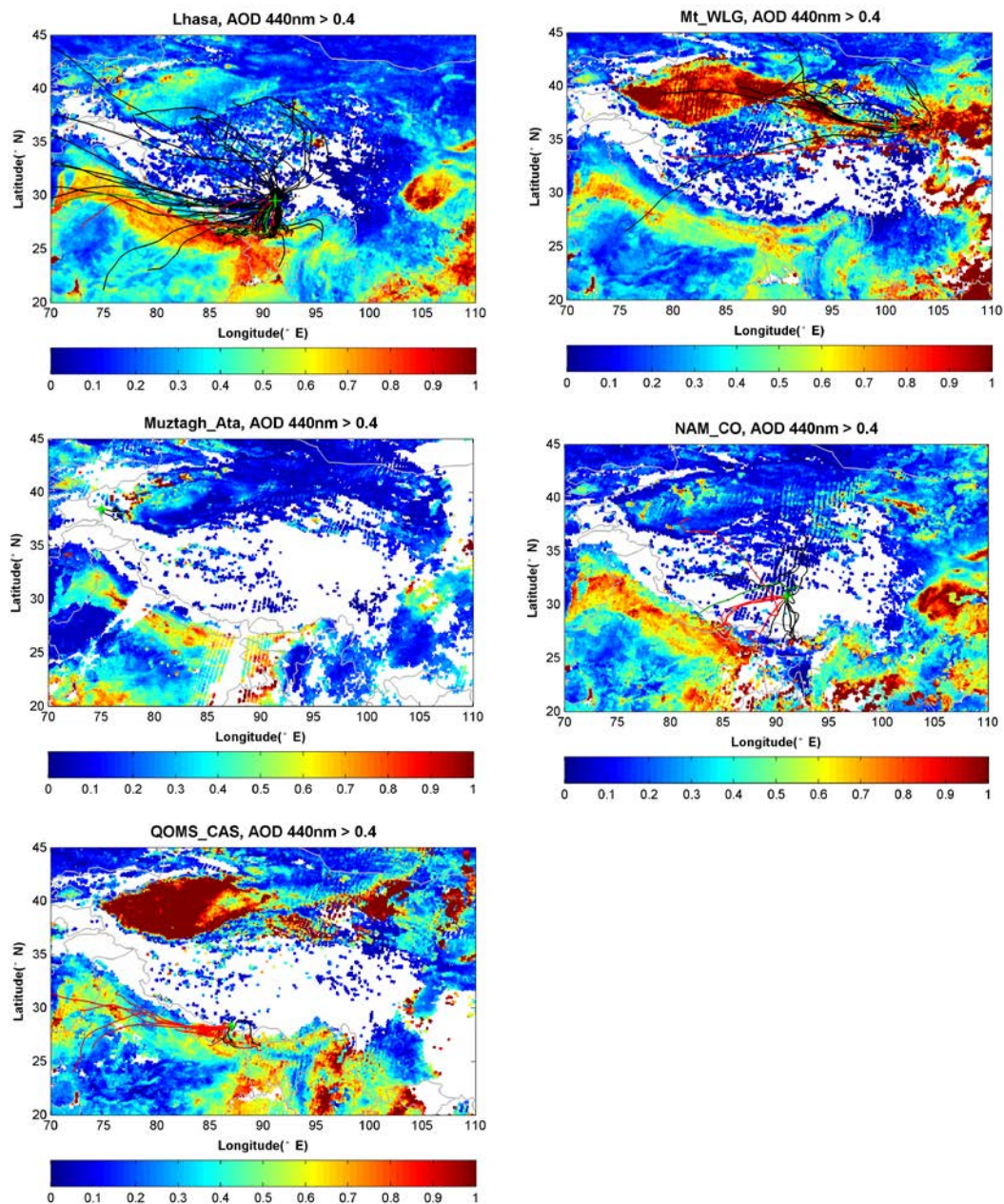
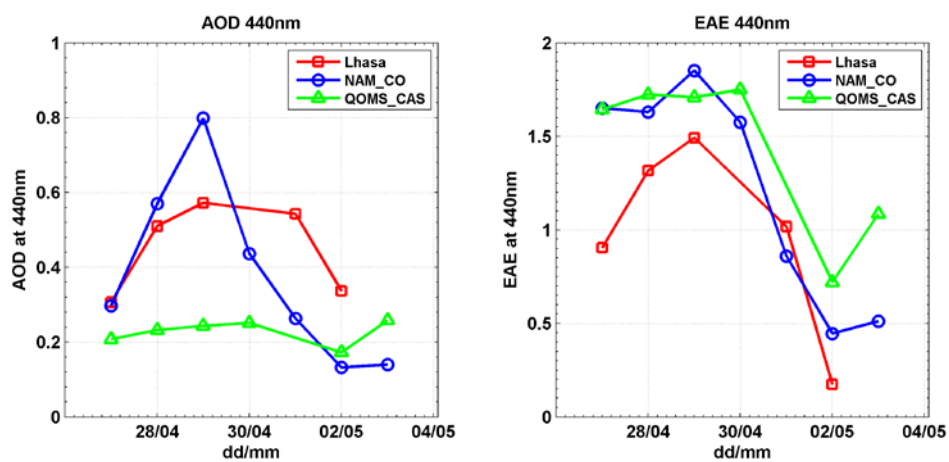


Figure 13. The back-trajectories ended at the five sites (10 m above ground level) on the TP overlaid by with the mean MODIS C6 AOD at 550 nm on the aerosol pollution day observed by ground-based CE318 (CE318 AOD > 0.4). Red stands for EAE > 1.0, black for EAE < 0.5, and green for EAE within 0.5-1.0.

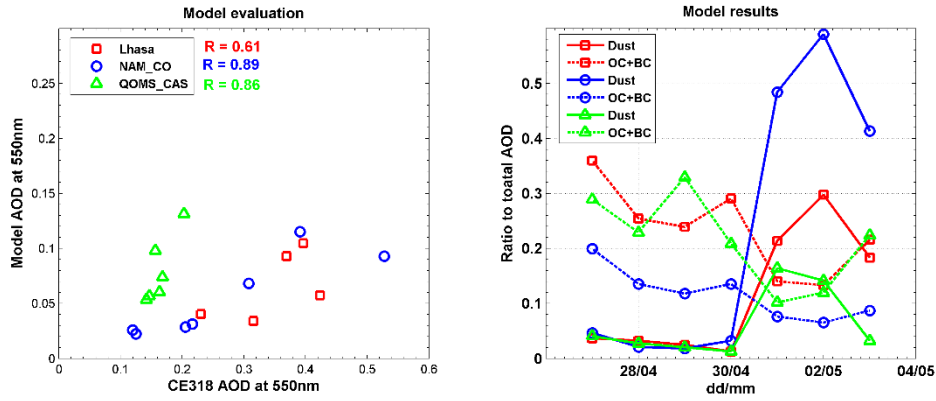


1

2 Figure 14. CE318 observed daily AOD at 440_nm and EAE during 27April-27, 2016 – 3May-3, 2016 at
 3 Lhasa, NAM_CO and QOMS_CAS.

4

1



2

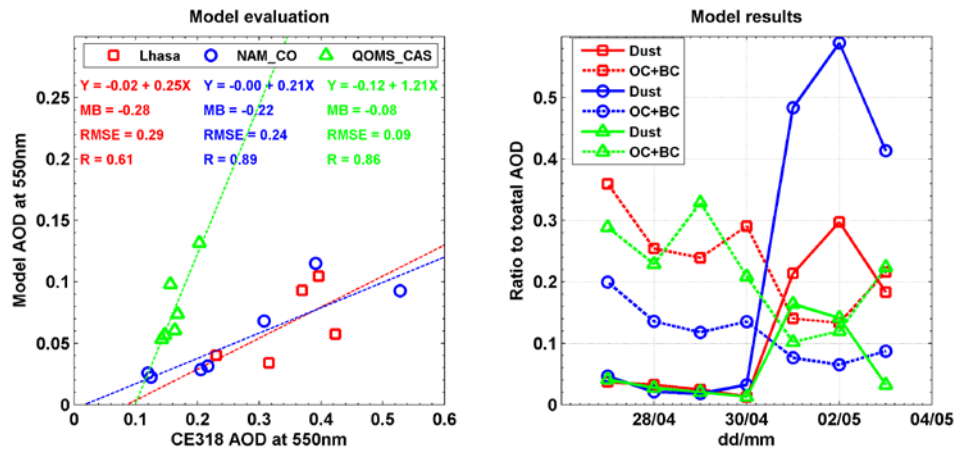


Figure 15. The GEOS-Chem model simulated the daily average AOD vs CE318 observed daily AOD at 550 nm and the ratios of dust or organic carbon (OC) and black carbon (BC) aerosol to the total AOD during 27 April–27, 2016 —3 May–3, 2016 at Lhasa, NAM_CO and QOMS_CAS. The statistical parameters used in the modal evaluation are the same as those in Figure 5.

7

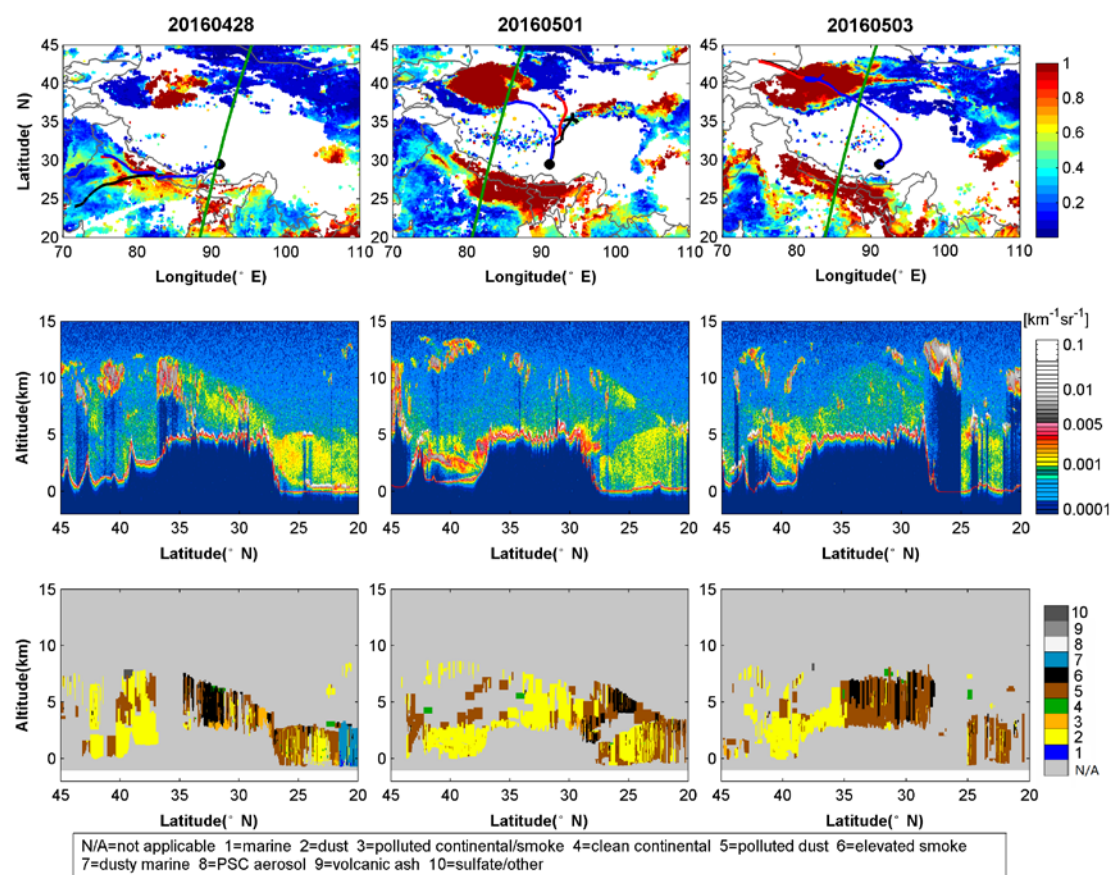


Figure 16. The MODIS C6 AOD at 550 nm and 72-hour back trajectories ended at Lhasa at three heights above the ground level (10 m in black, 500 m in red and 1000 m in blue lines) (the first row); the CALIOP-derived vertical profile of total attenuated backscatter at 532 nm (the second row); and the vertical feature mask of aerosol on 28 April, 1 May, and 3 May, 2016 over the ground track shown in the first row (green lines) (the third row).

1 Table 1. Site location and description.

Site name	Lat(° N)	Lon(° E)	Site description, observation days and period
Lhasa	29.50	91.13	Urban station over <u>on</u> the Tibetan Plateau, 3648_m a.s.l., 1554 days, 2007.05~2017.12
Mt_WLG	36.28	100.90	Mountain, 3816 m a.s.l., 314 days, 2009.09~2013.07
Muztagh_Ata	38.41	75.04	Mountain, 3674 m a.s.l., 84 days, 2011.06~2011.10
NAM_CO	30.77	90.96	Mountain, 4740 m a.s.l., 1061 days, 2006.08~2016.08
QOMS_CAS	28.36	86.95	Mountain, 4276 m a.s.l., 1623 days, 2009.10~2017.11

2

3

1 Table 2. Seasonal aerosol optical depth (AOD_{440nm}) and extinction Angstrom exponent (EAE_{440-870nm}) at
2 the five sites in [the](#) TP.

Site	AOD				EAE			
	MAM	JJA	SON	DJF	MAM	JJA	SON	DJF
Lhasa	0.16+0.	0.12+0.	0.10+0.	0.09+0.	0.72+0.	0.97+0.	1.11+0.	0.91+0.
	10	08	18	08	37	40	38	52
Mt_WLG	0.13+0.	0.14+0.	0.08+0.	0.08+0.	0.37+0.	0.65+0.	1.04+0.	0.58+0.
	16	07	11	07	38	40	80	69
Muztagh_Ata	NaN	0.14+0.	0.14+0.	NaN	NaN	0.73+0.	0.64+0.	NaN
		06	05			30	27	
NAM_CO	0.07+0.	0.06+0.	0.03+0.	0.03+0.	0.63+0.	0.62+0.	0.65+0.	0.78+0.
	07	04	05	01	44	45	32	43
QOMS_CAS	0.08+0.	0.06+0.	0.03+0.	0.03+0.	1.04+0.	0.76+0.	0.85+0.	1.10+0.
	06	04	01	02	38	43	51	67

3
4

1 Table 3. The percentages of EAE <0.5, 0.5-1.0, and >1.0 for high AOD observations at the five sites.

Site	N of AOD>0.4	% EAE<0.5/N	% 0.5<EAE<1.0/N	% EAE>1.0/N
Lhasa	655	60.6	3.4	36.0
Mt_WLG	290	73.4	0	26.6
Muztagh_Ata	5	100	0	0
NAM_CO	140	27.9	2.8	69.3
QOMS_CAS	59	23.7	0	76.3

2

3